Anatomical correlates and nomenclature of the chiropteran endocranial cast

Jacob Maugoust, Maeva Judith Orliac

The Anatomical Record

Anatomical correlates and nomenclature of the chiropteran endocranial cast

Journal:	*Anatomical Record*
Manuscript ID	AR-SI-BAT-22-0442
Wiley - Manuscript type:	Special Issue Article (Direct Via EEO)
Date Submitted by the Author:	14-Nov-2022
Complete List of Authors:	Maugoust, Jacob; Institut des Sciences de l'Evolution de Montpellier Orliac, Maeva; Institut des Sciences de l'Evolution de Montpellier
Keywords:	bats, brain, endocast, neuroanatomy, CT-scan

Title: Anatomical correlates and nomenclature of the chiropteran endocranial cast

Authors: Jacob Maugoust[1], Maeva Judith Orliac[1]

Affiliation: [1]: Institut des Sciences de l'Evolution de Montpellier, UMR 5554 Université de Montpellier, CNRS, IRD, EPHE, place Eugène Bataillon, 34095 Montpellier cedex 5, France

Corresponding author: Jacob Maugoust – jacob.maugoust@umontpellier.fr – +33467144944 (tel) – +33467143622 (fax)

Running title: Anatomy and nomenclature of the bat endocast

Manuscript correspondence: Jacob Maugoust, Université de Montpellier place Eugène Bataillon cc65, 34095 Montpellier cedex 5, France

Grant sponsor: Agence Nationale de la Recherche (ANR); Grant number: ANR-18-CE02–0003-01 (PI: M. J. Orliac)

Abstract

Bats constitute a diverse group of mammals highly specialized toward active flight and ultrasound echolocation. These adaptations reflect on their morpho-anatomy and have been tentatively linked to brain morphology and volumetry. Despite their small size and delicateness, bat skulls and natural braincase casts have been preserved in the fossil record and allow for investigating brain evolutionary history and inferring paleobiology. Recent progresses in imaging techniques now allow for virtually extracting internal structures, assuming that the shape of internal cavity casts reflects soft organ morphology. Such a correspondence is not straightforward regarding the braincase cast ("endocast"), because meninges and vascular tissues surround the brain in living organisms and the resulting endocast morphology is a mosaic of the marks left by all these tissues. The hypothesis that the endocast reflects the brain in terms of both external shape and volume has drastic implications when addressing brain evolution, but has been little discussed. To date, a single work addressed the correspondences regarding brain and braincase in bats. Here, taking advantage of the advent of imaging techniques, we review the anatomical, neuroanatomical, and angiological literature and compare the available knowledge of bat's braincase anatomy to a sample of endocranial casts representing most modern bat families. Such comparison allows for proposing a Chiroptera-scale nomenclature for future descriptions and comparisons of bat endocasts. This also encourages further works to formally test what is hypothesized here.

Keywords: bats - brain - endocast - neuroanatomy - angiology - CT-scan

Introduction

Bats, or order Chiroptera, are the only mammals that conquered the aerial environment by active flight (e.g., Anderson & Ruxton 2020). This extreme adaptation, associated to spatial navigation and hunting techniques using ultrasound echolocation (e.g., Teeling et al. 2016, Anderson & Ruxton 2020) implies spectacular modifications of their whole morpho-anatomy from the ancestral "mammalian bauplan". The conquest of the air has given bats a real evolutionary success: Chiroptera today account for a large part of the mammalian diversity (~21%, second most diverse mammalian order after rodents; e.g., Burgin et al. 2018) and show a wide array of flights and diets (e.g., Norberg & Rayner 1987). The specificities of bats ecology necessarily reflect on their central nervous system, and the brain has therefore been widely studied. Several works looked at the general morphology and diversity of the brain, with comparisons between and within chiropteran families (Schneider 1957, 1966, Henson 1970, McDaniel 1976, Hackethal 1981, Baron et al. 1996, Neuweiler 2000). However, most studies have focused on volumes and sub-volumes of the brain in order to correlate neural volumes to ecological traits (e.g., Mann 1961, Stephan & Pirlot 1970, Jolicoeur et al. 1984, Hutcheon et al. 2002, Safi et al. 2005, Dechmann & Safi 2009). Regarding the evolutionary history of the brain of bats, the fossil record is scarce and skull remains are rare (e.g., Brown et al. 2019). Still, there are exceptional three-dimensional preservation of skulls of extant and extinct families (e.g., Revilliod 1920, Barghoorn 1977, Hand 1997, Wilson et al. 2016) and few natural endocranial casts are available, providing access to some external features of the brain. Bat "fossil brains" were even among the first mammalian natural endocasts to be studied after paleoneurology basics were proposed by Edinger (1929, 1949). However, works on bats natural endocasts only briefly describe the external shape of the brains of extinct representatives of extant families (Edinger 1926,

1929, 1961, 1964a,b, Dechaseaux 1956, 1962, 1970, 1973).

In the last decades, investigations of sensory complexes of mammals were greatly enhanced by the advent of X-ray microtomography, giving access to internal structures without damaging specimens (e.g., Cunningham et al. 2014). An important effort has been put on the petrosal's bony labyrinth that houses the cochlea and the vestibular system and allows for inferring about audition and locomotion of species (e.g., Ravel & Orliac 2015, Pfaff et al. 2018). The braincase, housing the brain and associated structures, has also been described through studies on virtual endocranial casts, allowing for discussing brain morphology and volume (e.g., Jerison 1990). If the reconstruction of a bony labyrinth cast gives a trustful access to the soft tissues it houses (i.e., inner ear; e.g., Spoor et al. 1994, Orliac & O'Leary 2016), this correspondence is not straightforward regarding the brain. Indeed, meninges separate the brain tissue from the bones of the braincase in order to isolate and protect the former (e.g., Balanoff & Bever 2017). This non-neural structure of non-negligible thickness is likely to blur the correspondence between the actual external shape, and volume of the brain and the inner shape, and volume of the braincase (and of a braincase cast). Some works compared brain and endocranial cast size and shape in large mammals and highlighted important biases (Dechaseaux 1962, Lyras 2009, Benoit 2015, Bisconti et al. 2021) making inferences difficult on large-sized mammalian endocasts (unless exceptional cases or specific methodological adjustment). Other studies stated and/or showed that the brain reflects well on the inner braincase of small- and medium-sized mammals (Orlov 1961, Dechaseaux 1962, Kochetkova 1978). However, with global size decrease, bony structures and soft tissues get thinner and imprints left on endocasts get shallower, even though the thickness of meninges also decreases (e.g., Hackethal 1981), making the brain vs. endocast comparison process more difficult. Direct correspondence

between endocranial form and brain shape in bats was questioned by Schneider (1957). This work is the only study to compare brain morphology and endocranial anatomy in bats, and most of subsequent works regarding brain morphology in that group rely on this reference (e.g., Baron et al. 1996). Schneider (1957) postulates that endocranial bony ridges do not reflect cerebral foldings in bats, because cerebral foldings are not brain gyrification but blood vessels pathways imprints. This hypothesis has dramatic implications regarding the interpretation of bats endocranial casts and highlights the urge to consider the internal structures of the braincase altogether: bony walls, blood vessels, meninges, and the brain.

Micro CT-scan investigations now allow for accessing the endocranial cast of fossil bats and discussing the paleobiology and the evolutionary history of brain with time (Yao et al. 2012, Maugoust & Orliac 2021). However, reliable anatomical correlates of the endocranial cast is a necessary first step essential to exploit this complex structure in macroevolutionary or paleobiological studies, and previous attempts (e.g., Schneider 1957) have to be updated as imaging techniques improve. Here, we review more than 120 years of available literature on chiropteran cranial anatomy, angiology, and neuroanatomy to draw an exhaustive and general picture of structures likely to mark the inner braincase and we compare this “expectable framework” to the endocast morphology of a sample of 19 extant chiropteran species documenting 16 families. This morphological confrontation provides a first overview of the anatomical structures that can be observed on chiropteran endocranial casts and proposes a general tentative nomenclature that aims to homogenize the anatomical terms used.

Material, methods, and abbreviations

The comparative sample aims at documenting Chiroptera diversity and comprises 19 species documenting 16 extant bat families. In most cases, one representative per family is documented. Vespertilionids are here represented by two species in order to document the two main clades (e.g., Amador et al. 2018) of this very speciose family (almost 500 species, Burgin et al. 2018). Pteropodidae, sister-taxon to Rhinolophoidea, are documented here by three species; indeed, intrafamilial relationships of Pteropodidae remain problematic (e.g., Shi & Rabosky 2015, Almeida et al. 2016, 2020, Hassanin et al. 2020), we therefore retained species from three subfamilies that, together, always represent at least the basalmost pteropodid dichotomy. Several families could not be sampled because of lack of access to µCT-scan data; these are the Craseonycteridae (in Rhinolophoidea), the Myzopodidae (in Emballonuroidea or Noctilionoidea), the Furipteridae and Mystacinidae (in Noctilionoidea), and the Cistugidae (in Vespertilionoidea). Taken together, these five families not documented in our sample account for nine extant chiropteran species.

Of all 19 skulls, 14 have been downloaded on the Morphosource (Boyer et al. 2017) repository of Shi et al. (2018). The others specimens have been µCT-scanned using a SkyScan 1076 (for *Hipposideros armiger*) or a EasyTom 150 (all other species) at the University of Montpellier (Institute of Evolutionary Science of Montpellier) and come from different museum collections (Table 1). Endocranial casts have all been extracted from µCT-scans of skull using the software Avizo® 9.3.0 (Thermo Fisher Scientific-FEI) and its “lasso” and “brush” tools together with grayscale thresholds. Visualization was done using MorphoDig® (Lebrun 2018). Information about institution, taxonomy, scanning parameters, and scanning parameters are provided in the Table 1. All segmented endocranial casts are showed in the Figures 1 and 2 in dorsal, lateral right, lateral left, and ventral views (clockwise).

The anatomical abbreviations used here in the Figures 3-11 are listed below.

For brain parts: AON- anterior olfactory nuclei; c0- crus 0; CblrH- cerebellar hemisphere; CbrH- cerebral hemispheres; CC- caudal colliculi; cI- crus I; cII- crus II; Hc- hypophysis cast; IX- uvula (lobule IX); OB- olfactory bulbs; OT- olfactory tubercles; P- paraflocculus; PaL- paramedian lobule; PC- pyramidal copula; PiL- piriform lobes; PMOC- pons-medulla oblongata continuum; RC- rostral colliculi; TM- tectum of the mesencephalon; V- vermis; VI- declive (lobule VI); VIIa- tuber vermis (VIIa); VIIb- folium vermis (VIIb); VIII- pyramis (VIII).

For fissures, sulci, and imprints: Acs- anterocrural sulcus; Bs- bridge sulci; Cf- circular fissure; Cs- carotid sulcus; Ics- intercrural sulcus; ISs- infrasylvian sulcus; IHf- interhemispheric fissure; Its- intermediate sulcus; LPs- lateral parafloccular sulcus; Ls- lateral sulcus; LSCi- imprint of the lateral semicircular canal; Os- orbital sulcus; Pacs- paracrural sulcus; Pmf- paramedian fissure; Pocs- posterocrural sulcus; Ppf- prepyramidal fissure; PSs- pseudosylvian sulcus; Rf- rhinal fissure; Sf- secondary fissure; SLs- supralateral sulci; Ss- sylvian sulcus; SSs- suprasylvian sulcus; VIIs- VII sulcus; VI-VIIs- VI-VII sulcus; VPf- ventral parafloccular fossa.

For braincase openings: AOPC- anterior opening of the pterygoid canal; BF- basicochlear fissure; Ca- communicant aperture; CACF- caudal alisphenoid canal foramen; CCc- carotid canal cast; CF- carotid foramen; CP- cribriform plate of the ethmoid; Da- dorsal aperture; EF- ethmoidal foramen; EnCF- endocranial carotid foramen; ExCF- extracranial carotid foramen; FM- foramen magnum; HF- hypoglossal foramen; JF- jugular foramen; OpF- optic foramen; OTF- orbito-temporal foramen; OvF- oval foramen; PF- postglenoid foramen; PMVa- posteromedioventral aperture; PW- pyriform window; RTrSa- rostral transverse sinus apertures; SCa - supracribriform aperture; SEVF- sphenorbital emissary vein foramina; SF-

sphenorbital fissure; TRF- temporal ramus foramen; Ua- unknown apertures; Va- various apertures.

For nerves and vessels casts: ABSRc- anterior branch of the superior ramus cast; CVc- connecting vessel cast; DCVc- dorsal cerebellar vein cast; DSSc- dorsal sagittal sinus cast; FNc- facial nerve cast; IAMc- internal acoustic meatus cast; MCAc- middle cerebral artery cast; MMRc- main meningeal ramus cast; MRc- meningeal rami casts; RTrSc- rostral transverse sinus cast; SRTc- superior ramus trunk cast; SSc- sigmoid sinus cast; TeSc- temporal sinus cast; TrSc- transverse sinus cast; VCNc- vestibulocochlear nerve cast.

For vascular structures: ABSR- anterior branch; BA- basilar artery ; BCV- brachiocephalic vein; CA- common carotid artery; CaS- cavernous sinus; CCA- caudal cerebral artery; CCoA- caudal communicant artery; CEV- capsuloparietal emissary vein; CiA- ciliary arteries; CoS- communicant sinus; DCV- dorsal cerebellar vein; DPS- dorsal petrosal sinus; DSS- dorsal sagittal sinus; ECA- external carotid artery; EEA- external ethmoidal artery; EEV- external ethmoidal vein; EJV- external jugular vein; EOV- external ophthalmic vein; ICA- internal carotid artery; IJV- internal jugular vein; IOA- infraorbital artery; IOR- infraorbital ramus; IOV- infraorbital vein; IR- inferior ramus; LA- lacrimal artery; LDA- large diploic artery; LDV- large diploic vein; LMV- longitudinal mesencephalic vein; LV- lacrimal vein; MCA- middle cerebral artery; MdR- mandibular ramus; MMR- main meningeal ramus; MTV- middle temporal vein; MV- maxillary vein; MxA- maxillary artery; OA- ophthalmic artery; OR- orbital ramus; oSEV- other sphenorbital emissary vein; oTrS- other transverse sinus; OTV- orbito-temporal vein; OV- orbital veins; oVA- other vertebral artery; PBSR- posterior branch; RCA- rostral cerebral artery; RCbA- rostral cerebellar artery; RTrS- rostral transverse sinus; SA- stapedial artery; SCV- subclavian vein; SEV- sphenorbital emissary vein; SOA- supraorbital artery ; SOV- supraorbital vein; SR- superior ramus; SS- sigmoid sinus; STA- supratrochlear artery; TeS-

temporal sinus; TR- temporal ramus; TrS- transverse sinus; VA- vertebral artery; VPS- ventral petrosal sinus; VV- vertebral vein.

Nomenclature

Maugoust & Orliac (2021) proposed a nomenclature of the endocranial cast structures in bats, based on Hipposideridae. An updated and augmented version of this nomenclature is provided here, to be relevant at the Chiroptera order scale.

Schneider (1957) describes the external aspect of the brain of several chiropteran species of various families (pteropodids, rhinolophids, phyllostomids, etc.) and summarizes its descriptions at the order scale, both regarding the brain macromorphology and the "cranio-cerebral topography" (which corresponds to the endocranial cast morphology in that work). Schneider (1966) also describes the brain of *Rousettus aegyptiacus* in details and provides outstanding high quality representations and descriptions of the brain together with a three-dimensional stereotaxic atlas (in transversal plane, as in other stereotaxic atlases published since [Schneider 1966, Baron et al. 1996, Bhatnagar 2008, Scalia et al. 2013, Washington et al. 2018, Radtke-Schuller et al. 2020], but also in parasagittal and in horizontal planes). Schneider's descriptions and figures are a tremendous contribution and are indubitably helpful regarding brain external morphology and endocranial casts studies. Actually, studies establishing the correspondence between soft tissues of the cranial cavity and the soft tissues leaving an impression on the inner face of that cranial cavity are incredibly rare. Comparative neurobiology studies often study brain in "too much" details to be directly applied to paleoneurology; internal structures of the brain cannot be studied in paleoneurology. Works such as those of Schneider (1957, 1966) therefore bridge a gap between comparative neurobiology and comparative anatomy of endocranial casts.

Henson (1970) reviews previous works on bat brains, providing supplementary illustrations (with a megachiropteran bat, *Eidolon helvum*, and a microchiropteran one, *Macronycteris gigas*) and summarizing what is known of bat brains, both in terms of macro- and micromorphology. McDaniel (1976) also describes extensively the external morphology of the brain of phyllostomid bats - even if it concerns one particular group in my clade of interest, its methodology may stand. Hackethal (1981) reviews what has been done regarding the cerebral and cerebellar morphology in whole mammals, order by order; if its discussion about the cerebral morphology in bats is a summary and a discussion of the previous works, his work about cerebellar morphology is way more complete, with numerous figures and an impressive anatomical content discussed family by family. These works highly complete the review of Baron et al. (1996, the main work used for bats brain by Maugoust & Orliac [2021]), who compiled a large dataset of brain metrics and shortly discussed about the brain of bats in an evolutionary framework. Unfortunately, Baron et al. (1996) described the external morphology of the brain to a quite lesser extent compared to the previously cited references.

Several vascular structures enter and/or exit the braincase and may leave a mark on the bony walls of the braincase. These marks can be either grooves along the vascular pathway or foramina pierced into/between bones. Tandler (1899) describes the cranial arterial system of mammals, including bats, and Grosser (1901) describes the vascular system of bats, including cranial arteries and vessels. Together, these two works give a large anatomical basis to work with. Then, several other studies worked on these grounds to complete anatomical observations and homologies (Buchanan & Arata 1969, Kallen 1977, Wible 1984, 1987, Diamond 1991, 1992, Wible & Davis 2000, Giannini et al. 2006).

We complete here the nomenclature of Maugoust & Orliac (2021) following mainly

Schneider (1957, 1966), Henson (1970) and Hackethal (1981) for the identification of the nervous structures, and Tandler (1899), Grosser (1901) and subsequent works for the identification of vascular structures. We use Anglicized terms of the Nomina Anatomica Veterinaria (NAV, 2017) or of the Latin terms of the previously cited articles if missing in the NAV. The main result of this nomenclature is the Figure 3, exhibiting an archetype of a chiropteran endocranial cast with all the (potentially) visible structures we identified.

I Neural structures (Figs. 3-7)

I.1 Major components of the chiropteran brain observed on endocasts (Figs. 3-4)

The brain of bats (as for vertebrates in general) is composed of: i) the prosencephalon, anteriorly (the "forebrain"), which is divided in a telencephalon and a diencephalon, ii) the mesencephalon, medially (the "midbrain"), and iii) the rhombencephalon, posteriorly (the "hindbrain"), which is divided in a metencephalon and a myelencephalon (e.g., Barone & Bortolami 2004). Most of these parts are visible individually on an endocranial cast, but finer anatomy is less obvious and used terms vary between publications; we here list and chose a name for all externally visible brain structures in bats.

The telencephalon represents a major part of the brain and is composed of the paleopallium ventrally and of the neopallium dorsally, both separated by the rhinal fissure (e.g., Smith 1902a; Dechaseaux 1962). The paleopallium is formed of (e.g., Pigache 1970; Fig. 4A): the **olfactory bulbs** at the anterior extremity of the telencephalon; the **anterior olfactory nuclei** ("regio retrobulbaris" in Schneider [1966]) which are the visible part of the olfactory peduncles (Cleland & Linster 2019); the **olfactory tubercles**; the **piriform lobes** ("pseudotemporallappen" in Schneider [1966]). According to Schneider (1957), the rhinal fissure is only embodied by the circular fissure, and the imprint on the lateral aspect of the

cerebral hemisphere often identified as the rhinal fissure is in fact a vascular impression. However, by looking carefully at Schneider's transversal sections (Schneider 1957, 1966), one can notice that he spotted the rhinal fissure a bit dorsally to a slight impression, where there seems to be a change in the nature of the pallium. For this reason, we do not follow Schneider's (1957) assumption (see also the 'Neopallial foldings and cortices' section) and we assume that a rhinal fissure can be detected on endocasts by a depression. Besides the olfactory bulbs, the paleopallium and the neopallium together form the **cerebral hemispheres**, or cerebrum (Fig. 4A). These hemispheres are separated from the olfactory bulbs by the **circular fissure**, and from each other by the dorsally visible **interhemispheric fissure**.

In the diencephalon, taking into account the thorough descriptions and figures of Schneider (1957) for modern taxa, we consider by default that the epiphysis is very unlikely visible in Chiroptera. Baron et al. (1996) found a particularly dorsally exposed epiphysis in *Dobsonia* species and in *Rhinolophus luctus* and *Rhinolophus trifoliatus.* Here (Fig. 2), no pteropodid endocast show an epiphysis, which may be covered by the confluence of the dorsal sagittal and transverse sinuses. *Rhinolophus luctus* endocast shows a bizarre pattern of structures between the cerebral hemispheres and the caudal colliculi; it is not obvious to locate the transverse sinus, whose identification is a key to identify the other (i.e., neural) structures. However, as the transverse sinus runs parallel and near to the posterior border of the cerebral hemispheres in other rhinolophids (Maugoust 2021, unpublished PhD), we parsimoniously consider the same situation for *Rhinolophus luctus*. The epiphysis is thus not visible on the endocranial cast of this taxon. The ventralmost diencephalic structure visible ventrally, the hypophysis, is visible on endocasts as the **hypophysis cast** (Fig. 4D). Following Schneider (1957), the safest way to identify this structure on an endocast is to locate the

dorsum sellae, the posterior border of the sella turcica (to where lies the hypophysis). Without clear imprint of dorsum sellae, other central, shallower, depressions may be erroneously interpreted as the hypophyseal fossa (Fig. 4B).

The mesencephalon is only visible dorsally as the **tectum of the mesencephalon**, that is variably covered by the cerebral hemispheres and the cerebellum (vermis and/or cerebellar hemispheres). As a result, the colliculi are more or less apparent on the external surface of the brain, and then retrieved on an endocranial cast (Fig. 4E). The **rostral colliculi** may be visible but are less frequently observed than the **caudal colliculi** in our sample, as well as in the sample of Schneider (1957). An important note is that the variation in the morphology of the colliculi casts, especially regarding the caudal colliculi, is not necessarily the mirror of a variation in the morphology of those colliculi; it is rather a variation in their covering (by cerebral/cerebellar hemispheres; Schneider 1957, McDaniel 1976). Schneider (1957) also explains that the caudal colliculi are often inflated and that exposed colliculi of bats may be caused by inflated caudal colliculi rather than because of non-expanded cerebral and/or cerebellar structures, joining the conclusions of Edinger (1964a).

The metencephalon is dorsally and laterally visible as the cerebellum, medio-laterally formed of the unpaired **vermis**, and of the paired **cerebellar hemispheres** and **paraflocculi** (Fig. 4C). Following Larsell & Dow (1935), Maugoust & Orliac (2021) postulated that the flocculi is very unlikely to be visible on the external brain, and thus on an endocranial cast. However, Schneider (1966) labeled a part of what Maugoust & Orliac (2021) would have attributed to the paraflocculus as the flocculus. This flocculus is located medioventrally compared to the paraflocculus, which is consistent with what is illustrated by Larsell & Dow (1935). Moreover, a cerebellar structure distinguishes from the paraflocculus on the frontal plane of the stereotaxic atlas of the *Rousettus aegyptiacus* brain (Schneider 1966: e.g.,

section 4-2-4). Hackethal (1981) also illustrates in most species a medioventral flocculus, of varying size. Contrary to Maugoust & Orliac (2021), we consider that the flocculus can be visible on the external aspect of the chiropteran brain. However, the delineation separating it from the paraflocculus is not retrieved in our endocast sample (Fig. 4G), and only the paraflocculus is visible (see also the 'Cerebellar foldings' section).

The exposed lobules of the cerebellar vermis on an endocranial cast as proposed by Maugoust & Orliac (2021) are congruent with the descriptions, schemes, and sagittal sections of Schneider (1957, 1966) and Hackethal (1981) and may fit, in fact, for the whole order: the anteriormost exposed lobule is the **declive (lobule VI)**, followed by the **tuber vermis (VIIa)**, the **folium vermis (VIIb)**, the **pyramis (VIII)**, and the posteriormost one is the **uvula (lobule IX)**. The sagittal sections of Schneider (1957, 1966) and Hackethal (1981) are, however, of great importance and help for the identification of cerebellar fissures and sulci on the vermis. Maugoust & Orliac (2021) proposed a third crus of the cerebellar hemispheres (the crus 0), ontogenetically developing from the declive (lobule VI), which is located anteriorly to the two other crura (the I and II, or anterior and posterior, crura), ontogenetically developing from the tuber and folium vermis respectively (Larsell & Dow 1935). In our chiropteran sample, the cerebellar hemispheres indeed may have more than a single groove, separating more than two sections (Fig. 4F). An issue is to identify them. Schneider (1957, 1966), Henson (1970) and Baron et al. (1996) do not compare the external anatomy of the cerebellar hemispheres; Schneider (1966) and Henson (1970) tentatively identify the crura of the hemispheres, but without such a thorough comparative work as for other brain structures (e.g., "olfactory brain", tectum of mesencephalon, vermis). On the other hand, Larsell & Dow (1935) pay more attention to the development of the whole cerebellum, its lobules and fissures/sulci, but in a single bat species. The only fully extensive

work (i.e., regarding both the structure and the taxonomic group) is that of Hackethal (1981), so we mainly base our identifications on it. According to Hackethal (1981), the cerebellar hemispheres may be composed of up to five lobules. The three most anterior of the five are the (previously defined on endocasts by Maugoust & Orliac [2021]) **crura 0, I, and II**. The two posteriormost lobules are the **paramedian lobule**, extending from the folium vermis, and the **pyramidal copula** ("copula pyramidis"), extending from the pyramis (Fig. 4F). The two latter lobules are more variously present and of varying shape, size, and position relatively to the three crura; we therefore use the term "crus" for the three former to mark the fact that these lobules are less varying across species. We also do not name the crus 0 a "lobulus simplex" as in Hackethal (1981) or in the NAV (2017) because it refers to an ancient lobule name of the vermis (e.g., see Larsell & Dow 1935), which we found both obsolete and confusing.

It has to be pointed out that the subarcuate fossa (which houses the paraflocculus and the flocculus) may not be fully formed by bone: for instance, the figure 72b of Schneider (1957) clearly shows a fibrous collagen membrane closing laterally the subarcuate fossa. On an endocranial cast, that kind of soft tissue is not preserved and therefore no limit can be reconstructed while dealing with bones only; the subarcuate fossa would appear as laterally open, which is in fact not the case in the living animal. The figure 72b of Schneider (1957) is (to our knowledge) the only section of a bat skull showing the paraflocculus. An interesting fact is that it does not show other structures comprised in the subarcuate fossa than the paraflocculus and the flocculus, and Schneider did not mention that other structures than these (such as vascular structures) may be present in this fossa. Even though a single figure and the absence of anatomical note is not enough to propose rules at the ordinal scale, we at least propose that the interpretations based on subarcuate fossa cast morphology have to

first consider that external apertures of that fossa (on the external wall of it) on skulls and fossils result from the decay of fibrous tissues rather than from vascular pathways, unless clear vascular links can be demonstrated. In the present sample, there generally are up to two apertures: one is located on the posteromedioventral aspect of the paraflocculus, and the other on its dorsal aspect. Both apertures can greatly vary in size, and generally connect with the sigmoid sinus cast dorsally and posteriorly. Due to the varying position of the petrosal in the skull (and therefore of the subarcuate fossa housing the paraflocculus), the **dorsal aperture** can open dorsomedially to dorsolaterally, always toward the sigmoid sinus cast. From another point of view, the direction of the opening of this structure informs about the rotation of the petrosal relative to the skull. The **posteromedioventral aperture**, on the other hand, quite less varies in its position and in the direction of the opening. Both apertures can be seen in lateral views, but both are best seen using 3D models (Fig. 4H): the dorsal aperture can be invisible in lateral view if it opens dorsomedially, and the posteromedioventral aperture has a stricter medial direction and is therefore still difficult to spot in lateral view.

Regarding the ventral surface of the metencephalon, Schneider (1957, 1966) and Henson (1970) provide high-quality illustrations showing that numerous structures appear on the ventral surface of the brain; Baron et al. (1996) underlined the prominence of these structures on their illustrations and point out that the distinction between the pons and the medulla oblongata is not clear. Accordingly, the area where the pons and the medulla oblongata are located on a brain is smooth in our endocasts sample; we keep the term of **pons-medulla oblongata continuum** defined by Maugoust & Orliac (2021) and we address its morphology without more details (see Fig. 4I).

I.2 Brain foldings visible on endocasts (Figs. 5-6)

I.2.a General remarks on the nature of brain foldings in bats

In his morpho-anatomical description of bat brains, Schneider (1957, 1966) points out that grooves on the brain surface can be erroneously referred to as pallial foldings, such as the rhinal fissure or neopallial sulci. He points out that an osseous crest and/or the imprint of a vascular structure are actually responsible of a sylvian-like groove. The studies of Schneider (1957, 1966) are the only studies (to our knowledge) to describe the inner surface of the bat braincase in details ("cranio-cerebral topography") and to compare it to the external surface of the brain. The following review works of Henson (1970), Hackethal (1981) and Baron et al. (1996) are therefore based on Schneider's observations.

Only Baron et al. (1996) identify a sylvian sulcus while clearly assessing that they follow Schneider's conclusions. In his study of the phyllostomid brain, McDaniel (1976) however observes real neopallial sulci: a "pseudocentral" sylvian-like (= central-like) sulcus that Schneider described as an inner osseous crest, and a more anterior sulcus that McDaniel did not name. Taking into account the review of Baron et al. (1996) (which takes into account the works of Schneider [1957, 1966]), Voogd et al. (1998) recognize on the external surface of the brain of some microchiropteran bats a rostral (= orbital) sulcus (which is probably the unnamed anterior sulcus of McDaniel 1976) and a suprasylvian sulcus, and a sulcus "which might be homologous to the sylvian sulcus of primates" in both microchiropterans and megachiropterans (as proposed by Maugoust & Orliac 2021).

Today, the terms used in the literature to name brain foldings at the chiropteran scale are heterogeneous: the interpretations of Schneider (1957, 1966) have been followed by works treating of brain morphology (Henson 1970, Hackethal 1981, Baron et al. 1996), whereas other interpretations have been proposed by Maugoust & Orliac (2021) based on

endocasts, meeting to some extent the brain review of Voogd et al. (1998). Since the review of Baron et al. (1996), some high quality atlases became available, even though they generally document phyllostomid species (*Desmodus rotundus* in Bhatnagar 2008; *Carollia perspicillata* in Scalia et al. 2013; the mormoopid *Pteronotus parnellii* in Washington et al. 2018; *Phyllostomus discolor* in Radtke-Schuller et al. 2020). Representatives of these genera are also figured by Schneider (1957). These atlases, together with various works published regarding the brain-skull interaction (Barron 1950, Welker 1990, Raghavan et al. 1997, Garcia et al. 2018), help in tackling Schneider's conclusions.

Schneider postulates that a slight imprint visible on endocasts is in fact induced by a vascular structure lying close to the rhinal fissure but not by the latter. However, on histological figures locating the transition area between the paleopallium and the neopallium on fresh brains (Schneider 1957: figs. 47, 57, 63, 64), the distinction is in fact difficult to see and, when visible, it may seem to be a bit lower than the arrow he uses to spot it, being at the level of a slight external imprint (Schneider 1957: figs. 57, 63) as well as on recent stereotaxic atlases. All the brains illustrated by Schneider (1957) exhibit some neopallial sulci, caused by ridges on the inner surface of the braincase. Those ridges are visible on histological sections (Schneider 1957: figs. 62-64) and consist in bony thickenings filled with marrow. Besides, recent stereotaxic atlases confirm that bats brain do exhibit true sulci, as McDaniel (1976) observed in several phyllostomid species.

What we propose only relies on the available literature and obviously needs further studies focused on bats and using modern techniques (such as diceCT, e.g., Anderson & Murat 2015, Gignac et al. 2016, Hedrick et al. 2018). However, this enables for revising most of the (scarce) literature regarding in detail the macromorphology of the bat brain, and to consider that the external impressions on endocasts are real pallial foldings, including a

rhinal fissure and neopallial sulci. Taking this into account, we follow and complete the sulcal pattern proposed by Voogd et al. (1998) and Maugoust & Orliac (2021).

I.2.b Neopallial foldings and cortices

The present definition of the main neopallial sulci relies on Maugoust & Orliac (2021), who adapted a general "primitive" mammalian scheme to hipposiderids bats. However, a substantial rider must be provided when a much broader phylogenetical framework is considered (Fig. 5A).

Almost every chiropteran specimen studied here shows, at least, one neopallial sulcus. As previously described in fossil hipposiderids (Maugoust & Orliac 2021), it is here referred to as the **sylvian sulcus**. This sulcus, formed by the **pseudosylvian sulcus** and the **suprasylvian sulcus**, arises from the rhinal fissure with a dorsolateral orientation (in lateral view) and then bends posteriorwards (Smith 1902a). The dorsoventral-most part (even bent a bit anteriorly in some cases), linked to the rhinal fissure, is the pseudosylvian part, while the posteriorly bent part is the suprasylvian part. Among the specimens of our sample (Fig. 5B), it is not rare to see a sylvian sulcus isolated from the rhinal fissure, and that is bent posteriorwards. We identify this part as the suprasylvian part of the sylvian sulcus.

Chiropterans exhibit various degrees of complexity of sulcation pattern, from very simple ones (e.g., rhinopomatids, with a single, short, and shallow sylvian sulcus, so-called "lissencephalic") to more complex ones (e.g., *Pteropus* species, with more than five sulci). The sylvian sulcus is the most frequently retrieved. On most complex endocasts, a **lateral sulcus** is also present: it is parallel to the sylvian sulcus, and dorsomedially located relative to it (Smith 1902a, Dechaseaux 1962). Depending on the cases (Fig. 5D), there can be either (1) a single straight sulcus linking the lateral and sylvian sulci, perpendicular to both of them and

roughly at the level of the dorsal convexity of the sylvian sulcus (Fig. 5D1-2), or (2) up to three more oblique and curved sulci linking the lateral and sylvian sulci (sometimes even seeming to extend from one or the other sulcus; Fig. 5D3). This or these sulci are called **bridge sulci**, as they "bridge" the lateral and sylvian sulci. In pteropodid species with no lateral sulcus (excepting *Casinycteris argynnis*; Maugoust 2021, unpublished PhD), there is always a short and straight sulcus located dorsomedially, arising grossly perpendicular from the sylvian sulcus. Depending on the cases, it may point anteriorly (being oblique; Fig. 5D1) or dorsally (being perpendicular to the sylvian sulcus; Fig. 5D2). The latter, dorsally pointing, isolated sulcus is very close in its shape and location to the perpendicular bridge sulcus (Fig. 5D3); we propose a homology between these two sulci. The bridge sulcus can thus be oblique or perpendicular, straight or curved, and it can be linked to the sylvian sulcus or to the sylvian and lateral sulci.

In some taxa (Fig. 5E), a sulcus arises from the sylvian sulcus more anteroventrally than the bridge sulcus and ventrally to the suprasylvian part of the sylvian sulcus. This sulcus generally points posteriorly or posteroventrally, and it can be flat or dorsally convex. Due to its position, we name it the **infrasylvian sulcus**: it arises from the sylvian sulcus and connects only it, and it is more ventrally located than the suprasylvian sulcus.

On most complex endocasts (Fig. 5C), there can also be one to several sulci located medially to the lateral sulcus, being perpendicular to it. Due to their varying number, we do not propose an identification for each and call them **supralateral sulci**.

An anteriorly located sulcus, not connected with the sylvian sulcus, is often retrieved (Fig. 5F). It parallels to some extent the circular fissure in lateral view, being more dorsally located than the latter. This sulcus is referred to as an **orbital sulcus** (Smith 1902a, 1903), as

previously described by Baron et al. (1996) and Voogd et al. (1998).

A sulcus is sometimes found (Fig. 5G) between the orbital sulcus and the area of sulcal complexification, grossly parallel to and of similar extent that the orbital sulcus. We name it **intermediate sulcus**. No clear homology can be found with a classical pattern (see the basal pattern figured by Maugoust & Orliac [2021]) and it is of varying position and connections; it is potentially not homologous between chiropteran species.

We decide to not use the gyral terminology of Dechaseaux (1962) adapted to hipposiderid bats by Maugoust & Orliac (2021) because: (1) the epithet of the terms may correspond to a primitive and/or carnivoran gyral pattern but not to a chiropteran gyral pattern, which is not convoluted (or not convoluted centrifugally), and (2) this nomenclature appears to be incomplete compared to that of some recent studies. In their stereotaxic atlas of *Phyllostoma discolor*, Radtke-Schuller et al. (2020) name the structural and functional areas of the brain of that species, even though they did not name the neopallial sulci. However, the correspondence between the brain of the species they describe and the brain of some chiropteran species is not difficult to establish and may be applicable, at least regarding the major areas that are grossly surrounded by similar sulci to those named here (Fig. 5A).

The **frontal** and **dorsolateral-orbital cortices** are anteriorly located: the frontal cortex is posteriorly bounded by the orbital sulcus, and the dorsolateral-orbital cortex is in its ventrolateral continuity. However, both areas are not separated by a sulcus (even though the frontal part seems to be the only of the two that is bounded posteriorly by the frontal sulcus), so we group them here and name this area the **fronto-orbital cortex**. Posteriorly to the orbital sulcus and dorsomedially to the sylvian sulcus is the **parietal cortex**, posteriorly

followed by the **occipital cortex**. Again, it is tricky to separate the parietal cortex from the occipital one, as the limit between them is not a sulcus: according to Radtke-Schuller et al. (2020), they are located on each side of the dorsal convexity of the sylvian sulcus (the parietal and occipital cortices being respectively anterior and posterior to it). As they cannot be clearly separated, we refer to them together as the **parieto-occipital cortex**. Below the sylvian sulcus are the **insular** and **temporal cortices** (sometimes also called auditory cortex [e.g., Washington et al. 2018] as it includes auditory nuclei). As previously, no clear sulcus separates them; the only way to distinguish them is that the temporal cortex is the most inflated part of the two. Moreover, the insular cortex generally refers to the insula, an area located near the rhinal fissure and where forms the basis of the sylvian sulcus, the pseudosylvia; it is thus the most ventral area of the two. We refer to both areas as the **insulo-temporal cortex**. It has to be noted that this insulo-temporal cortex resembles to some extent to the reuniens and arcuate areas of Maugoust & Orliac (2021), even though the insular cortex seems to encompass the ventral basis of the sylvian sulcus.

There are therefore three main neopallial areas: the fronto-orbital cortex anteriorly, the parieto-occipital cortex dorsally and the insulo-temporal cortex ventrally. In each, slight distinctions without clear limit can sometimes be inferred depending on the boundaries of each. The sulci separating these three areas are the orbital sulcus (regarding the fronto-orbital and the parieto-occipital cortices) and the sylvian sulcus with its posterior extent (regarding the parieto-occipital and the insulo-temporal cortices). If the orbital sulcus is absent and thus the fronto-orbital and parieto-occipital cortices cannot be distinguished, we refer to this area as the **fronto-orbito-parieto-occipital (FOPO) cortex**.

I.2.c Cerebellar foldings

Maugoust & Orliac (2021) proposed a nomenclature of the visible cerebellar structures on an endocranial cast in hipposiderids. Though still valid, the part of their nomenclature regarding the fissuration and the cutting of the cerebellum is however limited given that the cerebellar hemispheres are sometimes more complex in other chiropteran bats. We intend to complete it at the Chiroptera scale here.

The vermis and the cerebellar hemispheres may be separated by a groove of variable depth, the **paramedian fissure**. We consider this groove as a fissure because it separates two main units of the cerebellum (i.e., the vermis and the considered cerebellar hemisphere). The paramedian fissure can be a varying width (Fig. 6A): we consider it to be narrow when a clear distinction can be made (Fig. 6A2); sometimes, there is a very shallow and gentle transition between the two structures, indicating a wider fissure (on endocasts; Fig. 6A1). Moreover, this fissure does not necessarily separate the vermis and the considered cerebellar hemisphere on their whole length; for instance, in the brain of *Rousettus aegyptiacus* figured by Schneider (1966), there is a clear discontinuity between vermian and hemispheric parts of the lobules VIIA, VIIB, and VIII but a clear lateral continuity of the lobule VI, so we expect this pattern to be likely found on endocasts.

Hackethal (1981) clearly confirms the lateral non-linearity of the lobules in bats proposed by Larsell & Dow [1935]. He also confirms that the declive may contribute laterally to the cerebellar hemispheres through the crus 0 of Maugoust & Orliac (2021). We therefore retain the terms of **anterocrural sulcus** separating the crura 0 and I, and the **intercrural sulcus** separating the crura I and II. Depending on the taxa (Fig. 4F), there can also be a supplementary contribution of the tuber vermis to the cerebellar hemispheres as the paramedian lobule and of the pyramis as the pyramidal copula. One can thus expect more than two sulci separating the lobules of the cerebellar hemispheres. Dow (1942) did not

provide any name for the sulci anterior and posterior to the paramedian lobule. Without other references, we name (1) **posterocrural sulcus** the sulcus separating the crus II from the following lobule (which can be either the paramedian lobule or the pyramidal copula) and (2) **paracrural sulcus** the sulcus separating the paramedian lobule from the pyramidal copula, which is of varying position (either posteriorly to the previous lobules, or posteroventrally to them).

According to Maugoust & Orliac (2021), endocasts also exhibit vermian counterparts of these cerebellar sulci, though they are not laterally continuous with them (Hackethal 1981). These counterparts are the **VI-VII sulcus** and the **VII sulcus**, separating the declive from the tuber vermis and the tuber vermis from the folium vermis respectively. More posterior grooves actually separate lobules from both the vermis and the cerebellar hemispheres and are therefore fissures. We retain the terms proposed on endocasts by Maugoust & Orliac (2021) of **prepyramidal fissure** and of **secondary fissure**, separating the folium vermis (lobule VIIb) and the pyramis (lobule VIII) and the pyramis and the uvula (lobule IX) respectively.

The uvula expands laterally: it is thought to contribute to the paraflocculus (Larsell & Dow 1935, Dow 1942) and it forms the flocculus (Dow 1942) on its lateral extremity. However, there is also a posterior lateral inflation of the vermis, mainly caused by the inflation of the vermian part of the uvula. Moreover, Dow (1942) and Hackethal (1981) demonstrated that there is no additional hemispheric lobule formed by the uvula. Thus, a lateral expansion of the posteriormost lobule of the vermis on our endocasts sample (e.g., Fig. 6B) is interpreted as a lateral inflation of the uvula.

Schneider (1957, 1966) and Hackethal (1981) demonstrated that a flocculus can be

ventrally exposed in bats. A posterolateral fissure may thus be visible on the ventral aspect of both the flocculus and the paraflocculus. However, on endocranial casts, such a delineation is not observed and the flocculus is even not decipherable at all throughout our chiropteran sample; only visible is the paraflocculus, without posterolateral fissure (e.g., Fig. 4G). On the ventral aspect of the paraflocculus, a depression is sometimes retrieved throughout our sample with associated sulci surrounding it with more variation (Fig. 6C). Thus, rather than defining a single sulcus associated with this as did Maugoust & Orliac (2021), we propose to define this structure as the **ventral parafloccular fossa**. The variation around this structure is too high to propose other identifications; the fossa itself can be a delineated fossa, or a broad sulcus deepening locally etc.

A delicate groove can also occur anteroventrally or ventrally (Fig. 6D), delineating a small platform; this groove is the **lateral semicircular canal imprint**. The ventral parafloccular fossa lies (antero) medially to this imprint. Some artificial openings are sometimes visible on the dorsolateral aspect of the paraflocculus, but they are more probably non-osseous walls of the subarcuate fossa (see 'Nervous imprints and exits' section).

On the lateral aspect of the paraflocculus, a sulcus may occur (especially in pteropodids; Fig. 6E): this sulcus is grossly anteroposteriorly oriented, but it is often bent at its anterior and posterior extremities. This sulcus is very close in its shape and location to the sulcus separating the dorsal and ventral paraflocculus illustrated by Schneider (1966). Larsell & Dow (1935) named it the lateral sulcus of the paraflocculus, but we simplify this here and name it the **lateral parafloccular sulcus**. Following the illustrations of Larsell & Dow (1935) and Hackethal (1981), it appears clear that the secondary fissure extends laterally but not up to the paraflocculus, and the lateral sulcus of the paraflocculus is not a lateral extension of the secondary fissure, as proposed by Smith (1902b) that Maugoust & Orliac (2021)

followed. Indeed, this lateral sulcus is not oriented in the same way (anteroposteriorly, or diagonally in the anterodorsal-posteroventral axis for the lateral sulcus; mediolaterally for the secondary fissure) and the lack of continuity between the two structures is clear in adults (Hackethal 1981: text-figs. I-X) and even more obvious during the ontogeny (Larsell & Dow 1935: figs. 15-17).

I.3 Nervous imprints and exits (Figs. 3, 7)

The main nervous opening retrieved on endocranial casts is the **foramen magnum**, posteriorly, that links the encephalon and the spinal cord (Fig. 7A).

The mesencephalon, the pons (from the metencephalon), and the medulla oblongata (from the myelencephalon) together form a functional unit which is the brainstem (e.g., Barone & Bortolami 2004). From this structure, 12 “cranial nerves” exit. These nerves exit the braincase through foramina generally visible in ventral view - and they can be reconstructed on endocasts. Skull apertures in Chiroptera have only been recognized for the genus Pteropus (Giannini et al. 2006) and therefore re-used in fossil hipposiderids (Maugoust & Orliac 2021). We rely on these works and therefore identify several apertures that serve, at least (see ‘Vascular structures’ section), as exit point for the cranial nerves. These apertures (e.g., Fig. 7A) are: the **cribriform plate of the ethmoid** (for the olfactory nerve, or cranial nerve I), separating the braincase from the nasal cavity; the optic canal, whose anterior opening is reconstructed as **the optic foramen** (for the optic nerve, or cranial nerve II), located between the presphenoid and the orbitosphenoid; the **sphenorbital fissure** (for the oculomotor, trochlear, ophthalmic and maxillary branches of trigeminal, and abducens nerves, or cranial nerves III, IV, V1, V2, and VI), a fusion of the sphenorbital fissure *sensu stricto*, or the rostral alisphenoid canal (“alar”) foramen, and of the round foramen;

the **oval foramen** (for the mandibular, branch of the trigeminal, nerve, or cranial nerve V3); the **internal acoustic meatus cast**, with both **facial** (VII) and **vestibulocochlear** (VIII) cranial **nerve casts**; the **jugular foramen** (for the glossopharyngeal, vagus, and accessory nerves, or cranial nerves IX, X, and XI); and the **hypoglossal foramen** (for the hypoglossal nerve, or cranial nerve XII).

To this pattern, some variation occurs among Chiroptera, mainly regarding the spheno-ethmo-orbital region (i.e., regarding the foramina of the anterior half of the ventral endocranial surface). First, the root of the trigeminal nerve often leaves an imprint on the ventral face of the braincase (e.g., Schneider 1957, 1966). On an endocranial cast, such root generally merges with the postero-medial border of the cerebral hemisphere, with still some further grooves marking the separation of the trigeminal nerve branches (Fig. 7B). Second, there can be a coalescence of some foramina with the sphenorbital fissure. The round foramen is likely to be always concerned (no separate round foramen has been reported in bats), and the optic foramen can be included too in this larger opening, leaving sometimes an irregular shape to the anterior border of the sphenorbital fissure (Fig. 7C). There is, to our knowledge, no case where the oval foramen also coalesces with the sphenorbital fissure.

In some taxa, the sphenorbital fissure narrows mediolaterally and can be visually subdivided (Fig. 7D). This is particularly true in some pteropodids, as already illustrated in *Rousettus aegyptiacus* (Schneider 1966: fig. D). Distinguishing which component of the nerve bundle (i.e., with nerves III, IV, V1 and VI) goes across one or the other aperture is tedious as there is little literature about the cranial nerve pathways in non-human mammals. As do Giannini et al. (2006), we follow what is known in the dog (Evans & Lahunta 2012: fig. 19-8): the abducent (VI) nerve has the medialmost course, the ophthalmic branch of the trigeminal nerve (V1) has the lateralmost one, the trochlear (IV) nerve seems to be lateral too, while it

is unclear for the oculomotor (III) nerve, even though it is more medial than IV and V1. In the studied species, the lateral subdivision of the sphenorbital fissure is generally wider than the medial one. We can confidently propose that the V1 branch exits through the lateral subsection of the sphenorbital fissure while the VI nerve exits through the medial one; we also propose that the IV nerve exits through the lateral subsection (as it is still somewhat lateral) while the III nerve exits through the medial one (together with the VI nerve, as they are both ocular motor nerve).

A small foramen sometimes lies just medially to the sphenorbital fissure, in general at the middle of the sphenorbital fissure length in the anteroposterior axis (or at mid-distance between the anterior extremity of the sphenorbital fissure and the round foramen when the latter is individualized), and it opens posteriorly in the palatine region. Such an aperture is found by Giannini et al. (2006) in *Pteropus*, Wible (2011) in *Ptilocercus* (Scandentia), and Muizon et al. (2015) in *Alcidedorbignya* (Pantodonta) for instance. It is related to the pterygoid (or "vidian") canal, through which run the pterygoid nerve (or "vidian" nerve, which is the uniting of the greater petrosal nerve that arises from the facial nerve, and the deep petrosal nerve) and the pterygoid branch of the maxillary artery (or "vidian" artery). This foramen corresponds to the **anterior opening of the pterygoid canal**. In bats, on an endocast, it is elongated and very small, being located on the medial side of the sphenorbital fissure (Fig. 7E).

II Vascular structures (Figs. 3, 8-10)

II.1 Arterial system (Figs. 3, 8A, 9)

II.1.a Summary of the major arterial vessels crossing the endocranial cavity in bats (Fig. 8A)

The main arteries that supply the head and the neck in mammals are the **common carotid artery** and the **vertebral artery** (e.g., Tandler 1899, Barone 2011, Standring 2016). At the basis of the head, the common carotid artery especially divides into the **internal** and **external carotid arteries** (e.g., Tandler 1899, Barone 2011, Standring 2016), which are of varying relative importance across mammals (Barone 2011). The vertebral and internal carotid artery generally supply the brain, while the external carotid artery supplies extracranial soft tissues (Tandler 1899, 1901). In bats, and especially in "microchiropterans", the vertebral artery is the main supplier of the brain and the contribution of the internal carotid artery is reduced (Kallen 1977, Wible 1984, Wible & Davis 2000), though several branches of the latter still cross the braincase.

The two paired vertebral arteries enter the cranial cavity through the foramen magnum, pierce the dura mater to lie below the brain (the medulla oblongata), then send a little artery posteriorwards (both paired contributions forming the ventral spinal artery) and unite to form the **basilar artery** (e.g., Grosser 1901, Barone 2011, Standring 2016). Besides short pontine rami, the unique basilar artery sends between the ears an artery (dividing in an internal auditive, or labyrinthine, artery and a caudal cerebellar artery) and then reach the anterior extremity of the brainstem (e.g., Grosser 1901, Barone 2011, Standring 2016). At this point, the basilar artery divides in two paired arteries: the **rostral cerebellar artery** (supplying the cerebellum, running along the ventral and posterior sides of the cerebellar hemispheres to end in the paramedian fissure) and the **caudal cerebral artery**, which shortly sends off the **caudal communicant artery**, forming the posterior side of the Willis, or cerebral arterial, circle (e.g., Grosser 1901, Barone 2011, Standring 2016). In bats, the caudal cerebral artery is the main cerebral artery (Grosser 1901, Kallen 1977) and supplies the cerebrum until reaching the olfactory bulbs region. In the vespertilionid *Vespertilio murinus*,

it then crosses the cribriform plate and reaches the septum narium (Grosser 1901). In rhinolophids (*Rhinolophus ferrumequinum* and *Rhinolophus hipposideros*), it divides in paired branches going above and under the callosal commissure: dorsal branches reach the medial side of the olfactory bulbs, and ventral branches further ascend anteriorly to the callosal commissure, go over the cribriform plate, enter the nasal cavity, and distribute themselves at the nasal septum (Grosser 1901) as medial ethmoidal rami (Kallen 1977). The caudal communicant arteries ultimately join the internal carotid artery during its intracranial course in these bats (see below; e.g., Grosser 1901, Barone 2011, Standring 2016). In the megachiropteran *Pteropus*, the caudal communicant arteries are very thick, to the point that the caudal cerebral arteries look like side branches of it (Tandler 1899).

During its proximal course, the internal carotid artery sends off several branches. It then approaches the ear region. In "microchiropterans", the internal carotid artery enters the tympanic cavity by a posterior carotid foramen, it sends off an important branch known as the **stapedial artery**, and it exits the tympanic cavity through an anterior carotid foramen (Wible 1987). Megachiropterans depart from this scheme: a course through the tympanic cavity with a stapedial artery is present during the ontogeny, but the stapedial artery then involutes and the internal carotid artery course changes and it ultimately stays outside from the tympanic cavity (Wible 1984). Such ontogenetical secondary loss is therefore assumed to be also a phylogenetic secondary loss, and is not rare across mammals (Wible 1987, Diamond 1991, Hitier et al. 2013). In "microchiropterans", the stapedial artery is a major branch and generally the internal carotid artery is thinner after sending it off (Grosser 1901, Wible 1984, 1987), and then necessarily thinner than the megachiropteran internal carotid artery while entering the cranial cavity (Wible 1984).

The "proximal" (Wible 1987) or "stem" (Diamond 1991) stapedial artery passes through

the obturator foramen of the **stapes** (e.g., Grosser 1901, Wible 1987). Either before (Wible 1984) or after this (Wible & Davis 2000), it sends off a short ramus posterior which eventually ends by anastomosing with the occipital artery (an earlier branch of the internal carotid artery in bats, Wible 1987). This ramus posterior is infrequently reported in angiological studies (Wible & Davis 2000), and though in some taxa it is present and complete (in the phyllostomid *Artibeus lituratus*, Buchanan & Arata 1969), it can lose its connection with the proximal stapedial artery (in the vespertilionid *Myotis*, Wible 1984) or be little developed and not reach the occipital artery (in the megadermatid *Lyroderma lyra*, Wible & Davis 2000). The stapedial artery then dichotomizes in two rami, the superior and the inferior ones (e.g., Tandler 1899, Wible 1984, 1987). This dichotomy apparently happens intracranially in bats in general (Wible 1984, 1987), the stapedial artery entering the braincase through the pyriform window (Wible 1984), but there are counter-examples (Wible & Davis 2000).

If originating extracranially, the **superior ramus** then enters the braincase through **various apertures** in bats (e.g., through a foramen in the tegmen tympani of the petrosal in *Lyroderma lyra* [Wible & Davis 2000], or in an unnamed space between the parietal and the squamosal in *Pteropus livingstonii* [Giannini et al. 2006]). This superior ramus then also ramifies in two branches: an anterior and a posterior one. The **posterior branch** gives off a **temporal ramus** (Buchanan & Arata 1969, Wible 1984, 1987, Diamond 1992, Wible & Davis 2000), that can be doubled to tripled in the megachiropteran *Pteropus* (Giannini et al. 2006), and that enters the bone in the parietosquamosal canal via a dedicated **temporal ramus foramen** (Grosser 1901, Buchanan & Arata 1969, Diamond 1992). In mammals in general, after giving off a temporal ramus, the superior ramus ends as the **large diploic artery**, which exits the skull through the posttemporal foramen, and then joins the occipital artery, a

branch of (generally) the external carotid artery (Wible 1987). This large diploic artery is absent in "microchiropterans" (Wible & Davis 2000) but it is present during the development of *Pteropus* (Wible 1987, Giannini et al. 2006), though it does not exit the skull. If present during early stages of extant megachiropterans, traces of this artery may be retrieved in fossil bats. Similarly, the temporal ramus could be absent in several megachiropterans, taking into account the absence of dedicated foramen in several taxa (Giannini et al. 2006). The **anterior branch** is generally bigger (Wible & Davis 2000) and runs anteriorly along the internal face of the braincase (e.g., Grosser 1901, Wible 1987, Wible & Davis 2000). Its intracranial course is often marked by a groove on the inner face of the braincase, the orbito-temporal canal (Giannini et al. 2006; also called "cranio-orbital sulcus" e.g., Wible 1987, Diamond 1991, Diamond 1992). During its intracranial course, it gives off several meningeal rami including a dorsally directed major one, named here the **main meningeal ramus**. Such ramus has also been designated as the middle meningeal artery, but Wible (1987) pointed out that the latter is actually a human composite feature formed by the derivative of the main meningeal ramus and by an extracranial stem growing out from the ramus inferior. Wible (1987) prefers to refer to meningeal rami for vessels only arising from the anterior branch of the superior ramus; since a main one is generally found in bats (Tandler 1899, Buchanan & Arata 1969, Giannini et al. 2006, see also after), such qualifier is used hereafter for commonness but further work is needed to assess its homology across bats. The anterior branch then enters in the diploë (Grosser 1901, Buchanan & Arata 1969, Giannini et al. 2006) and finally exits the skull through the **orbito-temporal foramen** (Giannini et al. 2006; also called "cranio-orbital foramen" e.g., Wible 1987, Diamond 1991, Diamond 1992). Though all "microchiropterans" seem to exhibit an orbito-temporal foramen, several pteropodids do not (e.g., the genera *Pteropus* and *Rousettus*) while several

others do, with therefore some intrafamilial variation (Kallen 1977, Wible 1984, Giannini et al. 2006). Once it enters the orbit, it becomes the **supraorbital artery** ("ramus") (Wible & Davis 2000). The orbital divisions of this ramus have been little described in bats; according to the mammalian-scale pattern (Wible 1987, Diamond 1991), it would first give rise to the **lacrimal artery**, then give the **external ethmoidal artery** and end in the **supratrochlear** ("frontal") **artery**. The lacrimal artery has however not been mentioned as being linked to the supraorbital artery but instead to the orbital ramus (see below, Tandler 1899, Wible 1984); it would then only give the external ethmoidal and supratrochlear arteries. The external ethmoidal artery then enters back into the skull through the ethmoidal foramen and seems to be separated from the supraorbital artery before the others, this separation occurring either intracranially in some "microchiropterans" (in the vespertilionid *Vespertilio murinus*, Grosser 1901) or extracranially in others (in the rhinolophids *Rhinolophus ferrumequinum* and *Rhinolophus hipposideros*, Grosser 1901). Buchanan & Arata (1969) also reported an anastomosis of the supraorbital artery with the orbital ramus (see below) for the phyllostomid *Artibeus lituratus*.

The **inferior ramus** of the stapedial artery, originating intracranially, exits the skull through the pyriform window (Wible 1987) and goes anteroventrally, finally joining a branch of the external carotid artery to form the **maxillary artery** (Wible 1987). Such connection is seen during the development in bats (Grosser 1901, Wible 1984) but is lost in adults, the ramus inferior remaining connected only to the stapedial system and being shorter (from totally absent to barely reaching the pyriform window; Wible 1984, Wible & Davis 2000) or it connects the maxillary artery and the superior ramus (Grosser 1901, Wible 1984, Giannini et al. 2006). The first case is generally saw in "microchiropterans" (Grosser 1901, Wible 1984, Wible & Davis 2000) whereas the second one is retrieved in megachiropterans (Tandler

1899, Wible 1984, Giannini et al. 2006).

In these pteropodids, the proximal stapedial artery does not just lose its connection with the inferior ramus: it fades during the development and also loses its connection with the superior ramus (Tandler 1899, Wible 1984, Wible 1987, Giannini et al. 2006), remaining as a short stump not connected to the internal carotid artery at best (Giannini et al. 2006), with obviously no proximal posterior ramus (Wible 1984). The two, inferior and superior, rami originating initially from the stapedial artery during the ontogeny then originate from the maxillary artery in adults. In these taxa, the inferior ramus is then just a communicant branch between the maxillary artery and the superior ramus (Wible 1984, Giannini et al. 2006). Therefore, we only retained the terms of "inferior/superior ramus" and of "anterior/posterior branch of the superior ramus" without saying the originating artery of these branches because of this uneven origin across all bats.

The maxillary artery then dichotomizes, giving off a **mandibular ramus** (going more ventrally) and an **infraorbital ramus**, which remains on the external ventral surface of the braincase (Wible 1987). The infraorbital ramus course is particular in bats compared with other placentals because it is often intracranial (Grosser 1901, Wible 1987), exiting the skull through the round foramen, which is often confluent with the sphenorbital fissure in bats (Buchanan & Arata 1969, Wible 1984, 1987, Wible & Davis 2000, Giannini et al. 2006). However, there is some variation in this intracranial course and counter-examples: it can enter the cranial cavity through the oval foramen (Wible 1984, 1987, Wible & Davis 2000, Giannini et al. 2006), a dedicated foramen separated by a bony bar from the oval foramen (Wible 1984), or through the alisphenoid canal (Buchanan & Arata 1969, Wible & Davis 2000), it can remain fully extracranial (in *Rhinolophus* and *Desmodus*; Grosser 1901, Kallen 1977, Wible 1984, 1987), and even have both intracranial and extracranial courses in a single

species (*Artibeus lituratus*, Buchanan & Arata 1969, Wible 1987). The infraorbital ramus then typically dichotomizes in an **orbital ramus** (or external ophthalmic artery) and an **infraorbital artery**, though there are sometimes more complex patterns with other branches sent off (e.g., the phyllostomid *Artibeus lituratus*, Buchanan & Arata 1969). In species with an intracranial course of the infraorbital ramus, this dichotomy generally happens before exiting the braincase (Wible 1984, 1987, Giannini et al. 2006). The ramus orbital then goes anteriorly, along the posterior surface of the orbit. In megachiropterans and some "microchiropterans", the orbital ramus then anastomoses with the ophthalmic artery (originating from the Willis circle, not specifically from the internal carotid artery) to give rise to **ciliary arteries** (megachiropterans: Tandler 1899, Wible 1984, Giannini et al. 2006; "microchiropteran" phyllostomid *Artibeus lituratus*: Buchanan & Arata 1969). Such pattern also exists in other "microchiropterans" but only occurs during the development, with a shift in the main supplier of the ciliary arteries from the ophthalmic artery to the orbital ramus during ontogeny (Wible 1984). Then, in the adult, either only the orbital ramus remains as the supplier of the ciliary arteries (Kallen 1977) and the ophthalmic artery fades during the development (Grosser 1901, Wible 1984), or the ciliary arteries become supplied by a branch of the anterior branch of the superior ramus, "before its division in external ethmoidal artery and supraorbital artery" in the rhinolophid *Rhinolophus ferrumequinum* (Grosser 1901), so probably intracranially. In some cases, the orbital ramus also becomes the supplier of arteries initially originating from the anterior branch of the superior ramus. In megachiropterans, there is a complete replacement taking part during the development: the anterior branch of the superior ramus first exits the skull as the supraorbital artery and supplies the external ethmoidal, lacrimal, and supratrochlear arteries, but then are anastomoses with the orbital ramus, and the superior ramus contribution is eventually lost

in the adult, the orbital ramus becoming the only supplier (Tandler 1899, Wible 1984, Giannini et al. 2006). In "microchiropterans" vespertilionids (in *Vespertilio murinus* and in *Myotis*; Grosser 1901, Wible 1984), such replacement is also partly observed, but there only the lacrimal artery becomes supplied by the orbital ramus (in one case for *Myotis*, the lacrimal artery becomes even supplied by the infraorbital artery; Wible [1984]).

The rest of the internal carotid artery (i.e., after sending off the stapedial artery) then enters the braincase (except some rhinolophids; Kallen 1977) through a carotid foramen (Grosser 1901, Wible & Davis 2000, Giannini et al. 2006) located either in the sphenoid in "microchiropterans" (e.g., lying on the posterior border of the sphenoid in *Lyroderma lyra* after Wible & Davis [2000]) or between the petrosal and the sphenoid in megachiropterans (Grosser 1901, Wible & Davis 2000). A short carotid canal has also been reported in megachiropterans (Tandler 1899) and in "microchiropterans" (Grosser 1901), but it may be subject to interpretation. It then crosses the cavernous sinus ("cavernous part" of its course) in the dural floor of the braincase and sends off several small branches during its course, supplying various structures (such as the hypophysis and the trigeminal ganglion) (e.g., Barone 2011, Standring 2016). It then (anteriorly) pierces the dura matter ("intracranial part" of its course), it links to the basilar artery by the caudal communicant artery, and turns back dorsally. While it bends, it sends off the **ophthalmic artery** (Tandler 1899, Grosser 1901, Barone 2011), which travels to the orbit through the optic foramen. This artery is present, though weak, in megachiropterans and some microchiropterans (*Desmodus*, Kallen 1977) and anastomoses with the orbital ramus (Tandler 1899, Wible 1984, Giannini et al. 2006), whereas it is lost during the ontogeny in "microchiropterans" (Grosser 1901, Wible 1984). We retain here the terms of "orbital ramus" and "ophthalmic" artery instead of "external/internal ophthalmic" artery used in the NAV (2017) mainly because of the non-

fully homology between the “ophthalmic” and “internal ophthalmic” arteries: the latter vessel generally arises from the internal carotid only before it connects to the caudal communicant artery (e.g., Barone 2011, Standring 2016), whereas in bats such connection happens first (Tandler 1899, Grosser 1901). Nonetheless, orbital ramus and ophthalmic artery in bats likely have the same function than the external and internal ophthalmic arteries of other placentals (Barone 2011). The remaining internal carotid artery then sends off other branches, especially the **middle cerebral artery** (or “arteria for Sylvian fossa” due to its location close to the sylvian neopallial sulcus; Robertson 1828, Tandler 1899, Grosser 1901, Schneider 1957), as well as arteries for the callosal commissure in megachiropterans (Tandler 1899; both left and right arteries ultimately connect each other and then close the Willis circle), and end in **rostral cerebral artery**, without rostral communicant artery. In “microchiropterans” vespertilionids, the rostral cerebral artery sometimes ends on the ventral surface of the olfactory bulbs (Grosser 1901). In two rhinolophids, the course is different: in *Rhinolophus hipposideros*, the rostral cerebral arteries anastomose with and finally join the caudal cerebral arteries close to the knee of the callosal commissure, whereas in *Rhinolophus ferrumequinum*, there is no such junction (Grosser 1901). Grosser (1901) interpreted such pattern as revealing that the internal carotid artery (as the rostral cerebral artery) would have first supplied the septum narium but would have then become more and more replaced in this role by the vertebral artery (as the caudal cerebral artery), with persistent anastomoses between both from times to times in rhinolophids.

II.1.b Arterial imprints on the endocast (Figs. 3, 9)

The vertebral artery enters the braincase through the foramen magnum. It has a short dural course, then it pierces it and lies below the brain. Of the two parts of this course, the first is the most likely to let an imprint on the endocranial surface of the basioccipital

because of its presence within the meninges. However, no paired trace anterior to the foramen magnum has been retrieved in our sample (Figs. 1-2). The two vertebral arteries then merge and become the basilar artery, with still an intracranial extradural course along the pons-medulla oblongata continuum. But probably due to this extradural location, and similarly to the vertebral arteries, no trace of the basilar artery has been found here (Figs. 1-2). At its anterior end, the basilar artery splits in eventually three main paired vessels.

The first is the rostral cerebellar artery, that, according to Grosser (1901), remains quite external to the brain, and runs around the cerebellar hemisphere to end between it and the vermis. Grosser does however not really describe the width of this artery, nor does he talk about the variation of this width along the artery's path. Here, traces of this artery could be seen around the cerebellar hemispheres but we believe that they would be erroneous: ventrally to the cerebellar hemisphere, there is a large imprint but it often opens laterally and it is more likely the cast of the sigmoid sinus (see below) because the latter has an intradural course, whereas the artery has an extradural one; posteriorly, it could be confused with a thin cerebellar hemisphere lobule but this would need the artery to be very wide, which has not been reported yet; dorsally, there is sometimes a thinner groove in the paramedian fissure but it is more likely the cast of the dorsal cerebellar vein (see below) because of its anterior rather than posterior (if it was the artery) extension. In the present sample, no trace of the rostral cerebellar artery has therefore been found (Figs. 1-2).

The second is the caudal cerebral artery, which course is much more internal to the brain. However, Grosser (1901) noted that this artery ends in the nasal cavity, reaching it by crossing the cribriform plate of the ethmoid (in vespertilionids) or by running over it (in rhinolophids). In the present sample, an aperture is sometimes found anterodorsally to the cribriform plate, being rather thin but generally continuous mediolaterally on the whole

olfactory bulbs width (Fig. 9A). Without naming it, Maugoust & Orliac (2021) first interpreted it as transmitting olfactory nerves as the cribriform plate does in fossil bats, but it actually seems unlikely after observing some extant species where it forms sort of a canal opening on the dorsal surface of the nasal bone. We propose to name it the **supracribriform aperture**, to designate its location over the cribriform plate (that can tilt depending on the taxa), and we hypothesis that the anterior end of the caudal cerebral artery could go through this aperture to reach the nasal cavity. However, such proposed name and function are very tentative; they obviously need further investigation and the name of this aperture may then change.

The third is the caudal communicant artery that connects the basilar artery to the internal carotid artery once the latter is in its "intracranial" course. This caudal communicant artery would then be retrieved antero-laterally to the pons-medulla oblongata continuum and would run anteriorwards to anteromedialwards. Once again, probably because of its intracranial extradural position, it seems unlikely to leave an imprint - and it does not in the present sample (Figs. 1-2). The mark of the internal carotid artery entrance should not be confused with a potential groove for the caudal communicant artery; of the two arteries, a sulcus for the internal carotid artery is more likely to cause such groove due to its intradural course while entering the braincase, whereas the caudal communicant artery remains outside the meninges.

Before entering the braincase, the internal carotid artery gives off a stapedial artery in "microchiropterans". This artery, after a course within the tympanic cavity, enters the braincase through the **pyriform window** (Wible 1984) and then dichotomizes in the superior and inferior rami (Wible 1987). Such dichotomy apparently also happens outside the braincase, within the tympanic cavity, in some "microchiropterans" (in the megadermatid

Lyroderma lyra, Wible & Davis 2000), whereas there is no more stapedial artery in megachiropterans. In both cases, only the superior ramus enters the braincase, and it does so through various apertures (see 'Summary of the major arterial vessels crossing the endocranial cavity in bats' section) and such entry point can be retrieved on an endocast (Fig. 9B). The superior ramus then dichotomizes in two anterior and posterior branches. The trunk of the superior ramus of the stapedial artery may be visible on the posterior wall of the piriform lobes cast (Fig. 9C), here called the **superior ramus trunk cast**, forming distally an angle with the proximal end of its anterior branch (see following). The inferior ramus may also have a short intracranial course in the sphenoid region in "microchiropterans", but no trace of it has been found here (Figs. 1-2).

The anterior branch of the superior ramus lies within the orbito-temporal canal; the orbito-temporal vein would lie there too, but it is likely to be absent (Diamond 1992), so we assume in the Figure 3 that the anterior branch of the superior ramus is the only of the two vascular structures filling this canal, and that the associated cast can be referred to as the **anterior branch of the superior ramus cast**, an "orbito-temporal canal cast" would end at the orbito-temporal foramen (see also below). It is now clear that such cast does not mark the position of the rhinal fissure in bats (Schneider 1957, 1966, Maugoust & Orliac 2021). It is however of varying morphology across chiropterans, depending on the skull organization and especially of the angle between the braincase and the rostrum (Fig. 9D). Arising from this branch are meningeal rami that can also mark the inner surface of the braincase (Fig. 9E). We propose that the **main meningeal ramus cast** is the first that can be recognized because it is the main one of the temporal rami, but also because it is the only that can be homologized throughout species (e.g., Wible 1987, Diamond 1991). Therefore, we simply label as **meningeal rami casts** the other branches arising from the anterior branch of the

superior ramus.

It has also to be highlighted that, in the pteropodids sampled here, the anterior branch of the superior ramus does not necessarily end as the main meningeal ramus: it continues anteriorwards similarly to “microchiropterans” (Fig. 9F). In these cases, the anterior branch of the superior ramus exits the skull by entering the diploë and then by crossing the orbito-temporal foramen; we warn here that what could be reconstructed as the anterior end of the anterior branch of superior ramus cast would therefore correspond to the diploic entrance of the anterior branch, not to an orbito-temporal foramen. Before or once entering the orbit, the anterior branch (or the supraorbital artery once out of the braincase) sends off an external ethmoidal artery (though this artery could also arise from the orbital ramus of the maxillary artery in megachiropterans) that enters back the skull through the **ethmoidal foramen**. As already described by Maugoust & Orliac (2021), such foramen is present on the lateral wall of the olfactory bulbs but it is difficult to delineate on endocranial casts.

The posterior branch of the superior ramus usually runs in the posttemporal canal (e.g., Wible 1993, Muizon et al. 2015), which is located between the petrosal and the squamosal, an area out of interest for a braincase endocranial cast (since such canal is not a “brain area”). The large diploic artery is therefore not visible on an endocranial cast (following previous section, it is highly unlikely to retrieve it at all) as well as the temporal ramus and its associated temporal ramus foramen.

Be it connected to the inferior ramus or not, the maxillary artery can also have an intracranial course, referred to as the infraorbital ramus. This ramus can enter within the braincase via different apertures piercing the alisphenoid bone. Of these, some are also crossed by cranial nerves, such as the oval foramen, the sphenorbital fissure, and the round

foramen (likely to be coalescent with the sphenorbital fissure in bats). In some bats, the infraorbital ramus however enters the braincase because it goes in alisphenoid ("alar") canal: its anterior opening ("rostral foramen") is coalescent with the sphenorbital fissure in bats, but the **caudal alisphenoid canal foramen** can be retrieved as an independent opening (e.g., *Lyroderma lyra*, Wible & Davis 2000). Such a foramen is located between the oval foramen and the sphenorbital fissure, both on the anteroposterior and mediolateral axes. It is therefore easily distinguished from the anterior opening of the pterygoid canal, which is located medially to the sphenorbital fissure, and generally of smaller size (Fig. 7E). However, it can be easily erroneously identified as a round foramen using only an endocranial cast. The only way to address this is to also consider the skull. Since no individual round foramen has been reported yet in chiropteran skulls, it may be safer to systematically consider isolated reversions of a coalescence of the round foramen with the sphenorbital fissure as being in fact a posterior opening of an alisphenoid canal while looking at natural endocranial casts or poorly preserved skulls. The caudal alisphenoid canal foramen can also merge with the oval foramen, yielding a much more elongated foramen than expected for an oval foramen only (Giannini et al. 2006; Fig. 9G). No case of coalescence of this foramen with the sphenorbital fissure has been reported yet; an absence of clearly delineated foramen implies that either it is confluent with the oval foramen or that it is absent, and this may be only solved by looking at the corresponding skull, if available. The whole endocranial sphenoid region is filled in the dura mater by the cavernous sinus, with several structures crossing it, and especially the branches of the trigeminal nerve (that may leave an imprint, see 'Summary of the major arterial vessels crossing the endocranial cavity in bats' section). Therefore, arterial vessels imprint on the bone are highly unlikely; the only possible manifestation of the infraorbital ramus would be the presence of a distinct anterior opening

of the alisphenoid canal.

The rest of the internal carotid artery, after (i.e., anteriorly to) sending off the stapedial artery, is considered to be a reduced structure in bats (Wible & Davis 2000); that would imply less and/or less marked endocranial imprints.

The internal carotid artery then enters the braincase through a **carotid foramen**, located within the (ali)sphenoid in "microchiropterans" and between the (ali)sphenoid and the petrosal in megachiropterans (Grosser 1901, Wible & Davis 2000, Giannini et al. 2006). In the present sample, an entrance of the internal carotid artery is not always retrieved - and when it is, the morphology varies (Fig. 9H). In some cases (Fig. 9H4), there is no apparent aperture between the petrosal and the (ali)sphenoid or within the posterior border of the sphenoid for the internal carotid artery; either it enters by an aperture we do not suspect, or it completely fades after sending off the stapedial artery (as in some rhinolophids; Kallen 1977). The megachiropteran condition, with a foramen between the petrosal and the (ali)sphenoid, proposed by Wible & Davis (2000) seem to also apply to "microchiropterans" according to our sample (Fig. 9H2-3). Apart from a "foramen", Tandler (1899) reported a "short canal" for the entrance of the internal carotid artery in megachiropterans; such pattern is also retrieved here in "microchiropterans", with a short canal within the sphenoid (Figs. 9H1, 9I). We name the reconstruction of such canal a **carotid canal cast**, and its two extreme apertures the **extracranial** and **endocranial carotid foramina**, only the latter being observed on an endocast. The endocranial carotid foramen can vary in its position: it is sometimes clearly separated from and posteriorly located to the posterior wall of the piriform lobe (Fig. 9I1), while some other times it is encompassed in the posterior wall of the piriform lobe and is very close to the oval foramen (Fig. 9I2). We are currently not able to distinguish the "carotid foramen" and the "endocranial carotid foramen" without having the

associated skull. We suspect the “microchiropteran” carotid foramen within the sphenoid observed by Wible & Davis (2000) (“anterior carotid foramen” in the vespertilionid *Myotis*, Wible [1984]) to actually be an extracranial carotid foramen, implying that in some “microchiropterans”, the internal carotid artery pierces the (ali)sphenoid with a carotid canal of varying length. On the other hand, the proper “carotid foramen” would then be the case of an aperture located between the (ali)sphenoid and the petrosal, and not within the (ali)sphenoid. Yet, to date, no study investigated the foraminal or canalicular nature of the entrance of the internal carotid artery in the “microchiropteran” braincase. Such distinction is therefore only tentative.

Independently from its entry point, the internal carotid artery may also leave an imprint on the endocranial surface of the (ali)sphenoid while entering the braincase. Such imprint has been previously reported in megachiropterans (Giannini et al. 2006) and is also retrieved here in pteropodids, as well as in some “microchiropterans” (Fig. 9H1-2). We name this groove a **carotid sulcus**. Such sulcus, shallower anteriorly, could mark the “cavernous” (i.e., intradural) part of the internal carotid path, then exiting the meninges. During its (following) “intracranial” course, the internal carotid artery joins the caudal communicant artery, sends off an ophthalmic artery (apparently only in megachiropterans), then a large (relative to the other branches already sent) middle cerebral artery (also called “sylvian fossa artery” because of its location) to end as the rostral cerebral artery. Across the present sample, the main mark that could be attributed to a contribution from the internal carotid artery is the **middle cerebral artery cast**, an anteriorly convex mark at the anterior third of the cerebrum whose ventral part sometimes extends to the sphenorbital fissure (Fig. 9J). The presence of the ophthalmic artery is likely to be retrieved only in megachiropterans, and it only would be as its exit point: the optic foramen. The rostral cerebral artery has an internal course and is

therefore unlikely to leave any imprint on the internal walls of the braincase. It could only be reported indirectly, while it joins branches of the caudal cerebral artery that eventually exit the skull through the supracribriform aperture.

However, there is one case with the cast of a channel branching the anterior extremity of the anterior branch of superior ramus cast to the ventral (i.e., proximal) part of the middle cerebral artery (*Sphaerias blanfordi*, Fig. 9K). An anterior continuity/skull exit of the anterior branch of the superior ramus has not been described in adult megachiropterans, but it has been in fetal and newborns (Wible 1984). It is especially the case of *Rousettus aegyptiacus*, that is present in our sample and that has been studied, at best, until the newborn stage (Wible 1984): here, it seems to extend anteriorly and reach the orbit and to then retain the newborn pattern described by Wible (1984: Fig. VIII-1), where there is a connection of the orbital ramus, of the ophthalmic artery, and of the anterior branch of the superior ramus. However, these connections happen within the orbit; here, it seems to happen within the braincase. Adding to this unlikelihood, if the connecting vessel is the ophthalmic artery, this would mean that the latter artery would be sent off after the middle cerebral artery, where it is thought to happen before in *Pteropus* (Tandler 1899, Grosser 1901) and in domestic mammals (Barone 2011). With such uncertainty, we therefore only name this cast as a **connecting vessel cast**.

II.2 Venous system (Figs. 3, 8B, 10)

II.2.a Summary of the major venous vessels crossing the endocranial cavity in bats (Fig. 8B)

The venous system received substantially less attention than the arterial one and that there were big time gaps between some works; therefore, we sometimes have to describe

several work results to then assess the correspondence between the described vessels.

In mammals, the blood from the head and the neck is mostly drained on each side by two paired veins, the **external** and **internal jugular veins**, but also on a minor part by the paired **vertebral vein** (e.g., Hegedus & Shackelford 1965, Barone 2011, Evans & Lahunta 2012). Across mammals, the relative predominance of the external or internal jugular vein is variable (Hegedus & Shackelford 1965, Barone 2011). In "microchiropteran" bats, according to Grosser (1901), the internal jugular vein firstly predominates, but this balance inverts during the ontogeny, the external jugular vein being stronger in the adult. In megachiropterans, both are of similar size (Kallen 1977). These three veins proximally connect with other veins to form the cranial ("superior") cave vein (e.g., Hegedus & Shackelford 1965, Barone 2011, Evans & Lahunta 2012). The connection order can vary across mammals. In general, the subclavian and jugular veins connect to form a brachiocephalic ("anonymous") vein (e.g., Hegedus & Shackelford 1965, Barone 2011, Evans & Lahunta 2012), though paired jugular veins can connect (forming a jugular trunk) before connecting paired subclavian veins (Barone 2011), then forming a bigger trunk. Then, the vertebral veins can join either the brachiocephalic veins, if there are, or the trunk connecting jugular and subclavian veins by joining with each costo-cervical vein or by merging together (Barone 2011). In vespertilionid bats and in megachiropterans, according to Grosser (1901), the external jugular vein first joins the **subclavian vein**, then does the vertebral vein (and the internal mammary vein), and then does the internal jugular vein, forming then a **brachiocephalic vein**, both uniting to form the cranial cave vein.

The jugular and vertebral veins all have intracranial tributaries, with therefore potential bony imprints. More importantly, several veins and sinuses first pour into the internal jugular vein and then switch to pour into the external one during the ontogeny (Grosser

1901). Especially, former intracranial tributaries of the internal jugular vein, that generally mostly drain the braincase (e.g., Hegedus & Shackelford 1965, Evans & Lahunta 2012, Standring 2016), eventually connect to the external system by means of emissary veins (Grosser 1901). Therefore, contrary to the arterial system, we start this summary of braincase venous structures from distal segments, then describing the vessels they are a tributary of.

An unpaired antero-posterior dural sinus is located dorsally to the brain, filling the interhemispheric fissure: the dorsal ("superior") sagittal sinus (Grosser 1901, Giannini et al. 2006, Barone 2011). Anteriorly, at the level of the circular fissure, the dorsal sagittal sinus connects with the paired rostral ("anterior") transverse sinus, located between the cerebral hemispheres and the olfactory bulbs, that Grosser (1901) further describes in vespertilionids and in rhinolophids. In vespertilionids, these sinuses drain veins for the lateral and dorsal faces of these cerebral hemispheres and olfactory bulbs, but also veins from the cribriform plate. In rhinolophids, each sinus even has two, lateral and medial, branches. The lateral part enters the diploë, exits on the ventral face to connect orbital veins, further joining the infraorbital vein, then the maxillary vein (paralleling the maxillary artery, with therefore an extracranial course in that case), and then the external jugular one. The medial, dural, part also reaches the base of the skull, receiving veins from the ventral surface of the brain, and then communicating with nasopharynx veins. Anteriorly to these rostral transverse sinuses, the dorsal sagittal sinus (as a thin vessel in rhinolophids, a large part of the blood going through the rostral transverse sinuses) ends by dividing itself in two branches; in rhinolophids, Grosser (1901) describes the dorsal sagittal sinus as running ventralwards along the cribriform plate's crista galli before dividing, but it is unclear regarding vespertilionids. The two vessels are designated as "sphenoidal emissary vein" ("emissarium

sphenoidale") by Grosser (1901), they exit the skull through either independent paired foramina near the optic ones (in vespertilionids) or through the sphenorbital fissure (in rhinolophids and megachiropterans), and then become "pterygoid veins" (or "pterygoid fossa veins"). Then, Grosser (1901) describes these veins as being connected to either the orbital veins, forming the infraorbital vein and pouring into the maxillary vein (in "microchiropterans"), or to the capsuloparietal emissary vein (in megachiropterans) and eventually to the external jugular vein, but also/or to the cavernous sinus (in vespertilionids, entering back into the skull through the sphenorbital fissure), and then eventually to the internal jugular vein.

A foramen located in the "sphenoid" (Grosser 1901) for such emissary veins has also been described in humans (e.g., Standring 2016) and tentatively in a fossil species (the artiodactyl *Leptoreodon*, Robson et al. [2022]). However, such foramen lies between the round and oval foramina instead than in the "sphenoid wing" (Grosser 1901: 326) and, in the human, such emissary vein instead connects the pterygoid venous plexus to the cavernous sinus intracranially (Standring 2016). In the dog (Evans & Lahunta 2012), there are emissary veins for the round foramen and for the sphenorbital ("orbital") fissure, joining respectively a vein in the alisphenoid ("alar") canal and ophthalmic veins and plexus to the cavernous sinus. None of these cases could represent a homologous to Grosser's chiropteran "emissarium sphenoidale" because of the foramen position and because of the structures these veins connect. Especially, the anteriormost ending of the dorsal sagittal sinus has been little described, and all the more for fossils, then it is difficult to assess any homology. As the only exception to our knowledge in fossils, Wible (2022) recently described two vessels resulting from the anteriormost division of the dorsal sagittal sinus in a cimolestan palaeoryctid, but they reveal to be frontal diploic veins, with an intra-osseous course and a

final exit of the skull in the orbit; in bats, such veins exit in the pterygoid fossa and by means of foramina. In the rat, Scremin (2015) shows a distinction between the parts of the dorsal sagittal sinus posterior to the rostral transverse sinus ("dorsal ["superior"] sagittal sinus" per se) and anterior to it ("superior olfactory sinus"). The latter then goes ventralwards and gives "inferior olfactory sinuses", some veins ("olfactory emissary veins") then exiting the skull below the olfactory bulbs as in bats, but then they come back into the skull to connect with the cavernous sinus. Such vessel could correspond to the "emissarium sphenoidale" and to the "pterygoid (fossa) vein" of Grosser (1901), but the fact that he says, for same taxa but not at the same moment of his description, that these veins reach the external jugular vein, either by pouring into the maxillary (in rhinolophids and vespertilionids "microchiropterans"; Grosser 1901:320,326) or the capsuloparietal emissary (in megachiropterans; Grosser 1901:334) vein, and the cavernous sinus (in vespertilionids; Grosser 1901:324) is confusing (do these veins split and really join both jugular veins or not?). Regarding Grosser's (1901) chiropteran "pterygoid vein", this term has been used in cetaceans and rodents to describe a vessel arising from the pterygoid muscles and branching with the maxillary vein and eventually the external jugular vein (Mutus (2001), Costidis & Rommel 2012). Similarly to Grosser's emissary vein and foramen, it is therefore difficult to consider Grosser's chiropteran "pterygoid veins" to be homologous with this cetacean and rodent one. With such uncertainty, we therefore neither use one of the previously cited names by Grosser (1901) to describe such vessel (and its associated foramen, when present) nor use other proposed names in the literature, and we propose to name it sphenorbital emissary vein, with its dedicated sphenorbital emissary foramen, pending further angiological work in bats.

Posteriorly, the dorsal sagittal sinus also dichotomizes as the paired **transverse sinus**

that is mediolaterally oriented and located between the cerebrum and the cerebellum (Grosser 1901, Diamond 1992, Giannini et al. 2006, Barone 2011, Evans & Lahunta 2012). According to Grosser (1901), the transverse sinus also drains two other veins: the great cerebral vein (that drains the anterior and inner part of the cerebrum) and the **longitudinal** mesencephalic vein (that drains the cerebellum, going between mesencephalic colliculi and reaching the anterior level of the cerebellar vermis and then dividing). Both veins generally open in the confluence of the two transverse and the dorsal sagittal sinuses, but sometimes they open in the proximal part of the transverse sinus, or even unite and form a short trunk which then opens in the sinuses confluence. Whereas it is unlikely to retrieve any mark on the inner wall of the braincase of the great cerebral vein due to its very internal position, the longitudinal mesencephalic vein seems more superficial in its proximal course (Grosser 1901: fig. 37) and may leave an imprint on endocasts.

Transverse sinuses, once separated, then run ventro-laterally (Grosser 1901). Each then divides in dural and diploic sections. The dural section quickly dichotomizes too, with a part going posteriorly around the otic capsule, having first a posteriorwards then a ventralwards orientation; this is the sigmoid sinus (Grosser 1901, Diamond 1992, Giannini et al. 2006, Barone 2011, Evans & Lahunta 2012). The other part of this dural section continues to run ventralwards and enters in the diploë at the base of the skull, joining the other, only diploic, section. The latter accompanies the trunk of the superior ramus (i.e., before it dichotomizes in anterior and posterior branch); though Grosser (1901) describes it as accompanying the "meningeal artery, a branch of the stapedial artery", it is still connected to a temporal ramus (Grosser 1901: textfig. 18). Once the two diploic parts join, they exit the skull together through the postglenoid foramen as Grosser's "emissarium temporale" that eventually join the external jugular vein. In megachiropterans, Grosser (1901) notes that, probably due to

the higher development of the cerebral hemispheres, the transverse sinus is located more posteriorly relative to the otic capsule: whereas it is located just medially to the postglenoid foramen in “microchiropterans”, it is anteroposteriorly between the postglenoid and jugular foramina in megachiropterans. In these bats, Grosser (1901) also note that the diploic-only canal paralleling the transverse sinus is not connected with the transverse sinus towards the dorsal sagittal sinus. In the phyllostomid Artibeus lituratus, Buchanan & Arata (1969) similarly observe a vein (the middle temporal vein) running in an intra-osseous canal and joining the transverse sinus just above the otic capsule, then exiting the skull through the postglenoid foramen, this vein then connecting the maxillary vein to form the external jugular vein. Finally, Giannini et al. (2006) describe the transverse sinus as dichotomizing above the otic capsule to give a sigmoid sinus and another trunk that shortly also dichotomizes in a superior (“dorsal”) petrosal sinus and in the capsuloparietal emissary vein, the latter being in a sulcus, then in an intra-osseous canal (the temporal canal), then exiting through the postglenoid foramen. It appears quite clear the emissary vein exiting the postglenoid foramen and joining the external jugular vein that Grosser (1901) named “emissarium temporale” actually represents the capsuloparietal emissary vein (e.g., Diamond 1992, Wible 1993). This vein is also called “retromandibular vein”, “postglenoid vein”, or “parietosquamosal vein”; we keep the term “capsuloparietal emissary vein” because it is the ontogenetically original structure giving rise to this vein according to Diamond (1992), and because it better accounts for the function of this vein (i.e., connecting extracranial and intracranial veins). The two former components of this vein described by Grosser (1901) are therefore not exactly the capsuloparietal emissary vein: there is a dural then diploic section (the “capsuloparietal emissary vein” described by Giannini et al. [2006] in megachiropterans) and the fully diploic section, that is sometimes dorsally linked to the

transverse sinus but sometimes not (Grosser 1901). The dural-diploic vessel, sister-branch to the sigmoid sinus, filling a sulcus and then the temporal canal, is therefore called a **temporal sinus** (Giannini et al. 2006); such name is also used in descriptions of veins in the dog (Reinhard et al. 1962, Evans & Lahunta 2012) and other domestic mammals (Barone & Bortolami 2004, Barone 2011). For the fully diploic vessel (i.e., not always communicating with the transverse sinus), we keep the term of **middle temporal vein** that Buchanan & Arata (1969) used.

Other vessels have been reported in mammals to branch to the transverse sinus and/or to the sister branch of the sigmoid sinus once the transverse one dichotomizes. Though Grosser (1901) did not further describe the superficial vascularization of the cerebellum, other works in mammals highlighted the presence of a (paired) **dorsal cerebellar vein**, located between the vermis of the cerebellum and the cerebellar hemispheres (Barone & Bortolami 2004), filling the paramedian fissure, and connecting to the transverse sinus before it dichotomizes ventrally. Such vein could be present in bats. Two venous branches arising from the sister branch of sigmoid sinus generally accompany endocranial arteries: a **large diploic vein** ("vena diploëtica magna"; "parietosquamosal vein" in Diamond [1992]) joins and parallels the large diploic artery, and another vein joins and parallels the anterior branch of the superior ramus (be it of the stapedial or of the maxillary artery; Butler 1948, Diamond 1992). The latter branch is sometimes named "cranio-orbital sinus", referring to the bony structure housing it, the cranio-orbital sulcus; such sulcus is here named orbito-temporal canal, so this venous branch is called the **orbito-temporal vein** (following Wible 2010, Muizon et al. 2015, Martinez et al. 2019). It is unclear whether these two latter veins are present in bats. It is already unclear whether there is a large diploic artery, and when considered present, the venous contribution may be quite smaller to absent (Diamond 1992,

Wible 1993). At least, Giannini et al. (2006) reported a short and closed canal for both large diploic artery and vein during the development of the megachiropteran *Pteropus*. Regarding the orbito-temporal vein, it seems that the orbito-temporal canal is largely, if not fully, filled by the anterior branch of the superior ramus of the stapedial artery (Wible 1987, Diamond 1992). Still, since its presence/absence in bats has not really studied, we carefully do not consider it as absent here. Considering a more global mammalian-scale level, the orbito-temporal vein follows the path of the anterior branch of the superior ramus and then exits the skull toward the orbit through the orbito-temporal foramen. While trying to propose homologies of human veins for other mammals, Diamond (1992) names this segment the periorbital vein; in a purpose of homogenization based on relative location of vascular segments, we call it a **supraorbital vein**. This vein anastomoses with the external ophthalmic vein in the back of the orbit (Diamond 1992). If the orbito-temporal vein manages to reach the orbit in bat, it may still be tiny according to Diamond (1992), so the orbital venous anastomosis may mostly rely on the contribution of the external ophthalmic vein. This orbital venous anastomosis drains several veins that grossly (i.e., to a lesser extent than in general, and with substantial inter-individual variation, according to Cheung & McNab [2003] in humans) parallel the orbital arteries (Cheung & McNab 2003, Standring 2016). To refer to the previously described orbital arteries only, it drains the **lacrimal vein** and then the **external ethmoidal vein** (traveling from the nasal cavity through the ethmoidal foramen; as for the arteries, there are two, anterior and posterior, ethmoidal veins in the human, but it may be safe to suppose that there is a single one in bats, as for the corresponding artery) (e.g., Cheung & McNab 2003, Evans & Lahunta 2012, Standring 2016).

An important paired intracranial sinus is the **cavernous sinus**, of variable venous to anastomotic aspect (Kallen 1977). In mammals in general, it is located on the ventral surface

of the braincase: it surrounds the hypophysis (with both cavernous sinuses on each side, and intercavernous sinuses connecting them anteriorly and/or posteriorly to the hypophysis; Grosser [1901]) and several structures cross it, of vascular (such as the internal carotid artery) or neural (such as the cranial nerves III to VI) natures (e.g., Barone & Bortolami 2004, Barone 2011, Wible 2011, Evans & Lahunta 2012, Standring 2016). Anteriorly, the cavernous sinus drains other venous structures outside the braincase; they join at the level of the sphenorbital fissure to form this cavernous sinus (e.g., Diamond 1992, Wible 1993, Wible 2011, Evans & Lahunta 2012). Of the various structures forming it is the superior (in humans; e.g., Diamond 1992, Cheung & McNab 2003, Standring 2016) or **external** (in the dog; e.g., Evans & Lahunta 2012) **ophthalmic vein** (e.g., Grosser 1901, Diamond 1992, Wible & Zeller 1994, Cheung & McNab 2003, Palermo 2013). Posteriorly, the cavernous sinus connects with other vessels. First, it connects to another branch of the sister branch of the sigmoid sinus (reported in megachiropterans, Giannini et al. [2006]): the **dorsal** ("superior") **petrosal sinus**, which runs on the anterior aspect of the petrosal (e.g., Diamond 1992, Wible 1993, Barone & Bortolami 2004, Giannini et al. 2006, Barone 2011). Second, a vessel sometimes connects the cavernous sinus with the capsuloparietal emissary: the **communicant sinus** (Diamond 1992), which is generally accompanied intracranially by the arterial inferior ramus. In *Lyroderma lyra* (Wible & Davis 2000), the communicant sinus exits the braincase by the aperture crossed by the superior ramus (which is, in this species, a foramen in the tegmen tympani of the petrosal) and then goes back in the braincase through the pyriform window, then joining the cavernous sinus. In this species, the inferior ramus is a short stump, at most reaching the pyriform window (Wible & Davis 2000). Diamond (1992) did not find a communicant sinus in the phyllostomid *Carollia perspicillata*; this sinus may be variably present in bats. Of these two vessels, the communicant sinus appears to branch more

anteriorly than the dorsal petrosal sinus (Wible 1993, Wible & Davis 2000). The cavernous sinus posteriorly dichotomizes and pours the paired **ventral** ("inferior") **petrosal sinus** (e.g., Grosser 1901, Wible 1993, Barone 2011, Muizon et al. 2015, Standring 2016); each is located on the ventral aspect of the petrosal and remains inside the braincase in bats (even if it variously fills the basicochlear fissure; Giannini et al. 2006). Each ventral petrosal sinus posteriorly joins the sigmoid sinus and, together, form the internal jugular vein that exit the skull through the jugular foramen (Grosser 1901, Hegedus & Shackelford 1965, Diamond 1992, Giannini et al. 2006, Barone 2011, Evans & Lahunta 2012). In megachiropterans, though, the sigmoid sinus also (and mainly) exits the skull through the foramen magnum, pouring in the vertebral vein (Giannini et al. 2006).

II.2.b Venous imprints left on the inner braincase (Figs. 3, 10)

The dorsal sagittal sinus is sometimes visible as a **dorsal sagittal sinus cast** between the two cerebral hemispheres and within the interhemispheric fissure. Several endocranial descriptions within mammals labeled such cast "by default" as the interhemispheric fissure (e.g., Ferreira et al. [2022] with labels of the "superior sagittal sinus" on the interhemispheric fissure [their fig.4d] and on the actual sinus cast [their figs.4a and 4g]); we warn here that this cast is not often visible, as highlighted by the present sample (Figs. 1-2), and the interhemispheric fissure and the dorsal sagittal sinus cast have to be distinguished.

Anteriorly, the dorsal sagittal sinus first sends off paired rostral transverse sinuses, that run laterally along the circular fissure. The **rostral transverse sinus cast** is retrieved here (Fig. 10A); as for the dorsal sagittal sinus cast, the sinus cast and the fissure have to be distinguished. If then exiting the skull (see 'Summary of the major venous vessels crossing the endocranial cavity in bats' section), some foramina have been retrieved here that may

correspond to the exit point of these sinuses (Fig. 10B). They are located just anterolaterally to the sphenorbital fissure, anteroposteriorly between the unknown foramen #1 (when present) or the optic foramen (when individualized) and the sphenorbital fissure. When present, such foramen is generally small (Fig. 10B1), though its size and even maybe the number of apertures can vary (Fig. 10B2). Since such identification is tentative and since there seem to not be necessarily a single foramen, we refer to these as **rostral transverse sinus apertures**.

At its anterior extremity, the dorsal sagittal sinus dichotomizes in two sphenorbital emissary veins. Though this would rather happen on the ventral aspect of the olfactory bulbs (Grosser 1901), this dichotomy point remains unclear. Still, in the present sample, no anterior continuation of the dorsal sagittal sinus over the olfactory bulbs, no dichotomy and no paired vessels running anteroposteriorly on the ventral side of the olfactory bulbs have been noted (Figs. 1-2). However, the sphenorbital emissary vein then exits the skull either through the sphenorbital fissure or through a dedicated foramen near the optic ones. Here, we observed apertures that could correspond to these **sphenorbital emissary vein foramina** (Fig. 10C). Such foramen is generally located posteriorly on the ventral aspect of the olfactory bulbs (i.e., just anteriorly to the circular fissure). This foramen could be (erroneously?) identified as an optic foramen (Fig. 10C1): its position is much more anterior than expected for an optic foramen, and in some cases, a "true" optic foramen is also present (Fig. 10C2). It is generally retrieved as a large foramen (close to the oval foramen size for instance). It has however to be noted that this foramen could correspond to the suboptic foramen (Cartmill & MacPhee 1980) which "carries an [interorbital] vein connecting the ophthalmic veins" and is located "immediately posterior[ly] to the olfactory chamber" (Butler 1948). Since such structure have, to date, not been reported in bats, we prefer to

consider that the sphenorbital emissary vein cross this foramen, but this hypothesis still awaits further angiological work.

Consistently retrieved is the wide **transverse sinus cast**, delineating the posterior limit of the cerebral hemispheres (Fig. 10D). Its medial part may however be tricky to identify, as it passes near/over the rostral colliculi and the epiphysis according to Maugoust & Orliac (2021) (though we here consider very unlikely the epiphysis to be visible, see 'Summary of the major venous vessels crossing the endocranial cavity in bats' section). Evidences in several taxa of our sample (Fig. 10E) show that the medial course of the transverse sinus is anterior to the location of the rostral colliculi, clearly paralleling the posterior border of the cerebral hemispheres. This sinus then extends far laterally, along the anterior side of the cerebellar hemispheres. During its course, the transverse sinus receives proximally the dorsal cerebellar vein, which leaves an imprint in some taxa, the **dorsal cerebellar vein cast** (Fig. 10F). As previously, such cast has to be distinguished from the paramedian fissure. Though also having an intracranial extradural course, no cast for the mesencephalic longitudinal vein has been observed here (Figs. 1-2). The transverse sinus then splits in a dural and a diploic sections; the diploic one, the middle temporal vein, is unlikely to be retrieved here due to its location, though in skulls with damaged inner braincase wall it may be seen. The dural section then splits in a perpendicular and posteriorly located sigmoid sinus, which surrounds the petrosal dorsally and posteriorly, and the temporal sinus on the transverse sinus' continuation. Both **sigmoid sinus cast** and **temporal sinus cast** can be retrieved on the endocasts of our sample (Fig. 10G).

Pteropodids of our sample do not show a cast of a vessel going from the sigmoid sinus toward the foramen magnum, which would highlight the presence of the sigmoid sinus contribution to the vertebral vein (Figs. 1-2). However, noticeable is that the sigmoid sinus is

often continuous with the posterior side of the cerebellar hemisphere: there is often a groove delineating each structure, but both are still continuous (Fig. 10H). Posteriorly, it is also often (but irregularly) continuous with the jugular foramen, where it exits and forms the internal jugular vein together with the ventral petrosal sinus. The temporal sinus, on the other side of the otic capsule, then quickly enters a canal within the bone which is variously closed among taxa, joining the middle temporal vein before exiting the skull as the capsuloparietal emissary vein through the postglenoid foramen (Fig. 10G). Grossly, such canal is still visible on the surface of the posterior wall of the piriform lobes in megachiropterans, while it is less visible to not visible at all in most other bats. The various veins likely to connect the temporal ramus during its intradural course (the large diploic vein, the orbito-temporal vein, the dorsal petrosal sinus) do not seem to leave any imprint on the endocasts (Figs. 1-2).

A fine cast often runs from the ventral end of the temporal sinus cast to the pyriform window (Fig. 10G), with sometimes the anterior branch of the superior ramus branching to it (Fig. 10G1) and even the trunk of the superior ramus crossing it before dichotomizing (Fig. 10G2). Observing µCT-scan slices of the corresponding skulls, it appears that this fine cast is not a bony suture (Fig. 10G3-4). The only structure with a dorso-ventral course dorsally to the pyriform window is the communicant sinus, but its course is extracranial. Here, looking at µ-CT slices of the skulls, it appears that this fine cast is not a groove on the inner wall of the braincase, it is a continuous thin opening. Without other solution, we hypothesize that the communicant sinus goes through this continuous opening, still not knowing if it crosses it or if it fills it. We therefore name this cast the communicant aperture, to refer to the communicant sinus. This hypothesis remains very tentative, since Wible & Davis (2000) reported a communicant sinus clearly exiting the braincase with the superior ramus through

the petrosal's tegmen tympani and then entering back in it through the pyriform window in the megadermatid *Lyroderma lyra*, and since Diamond (1992) did not retrieve this sinus at all in the phyllostomid *Carollia perspicillata*.

Ventrally are located the sinuses pouring into the internal jugular vein. On both sides of the hypophysis, sometimes also connecting before and/or after it, lie the cavernous sinus in the meninges. Though the sinus itself does not appear to be depictable on endocasts (Figs. 1-2), we suppose that its presence around the hypophysis can contribute to blur the delineation of the latter on the ventral face of the braincase (see Fig. 4D). Anteriorly, the cavernous sinus receives the contribution of the external ophthalmic vein, entering the braincase through the sphenorbital fissure. No other trace of this vein is found on the endocasts of our sample (Figs. 1-2). Posteriorly, the cavernous sinus splits in paired ventral petrosal sinuses. Each of these is located medially to the petrosal, variously filling in the **basicochlear fissure** but remaining within the braincase. Therefore, it is more the basicochlear fissure itself that can be viewed on the endocranial cast than the ventral petrosal sinus per se. This sinus then joins the sigmoid sinus to form the internal jugular vein and exit the skull through the jugular foramen.

A noteworthy point is that the different apertures surrounding the petrosal (the pyriform window, the carotid foramen, the basicochlear fissure, and the jugular foramen), through very different vascular and nervous features cross them (communicant sinus, stapedial artery, internal carotid artery, ventral petrosal sinus, sigmoid sinus, and cranial nerves IX to XI), can coalesce to varying degrees and vary in width (Fig. 10I). The basicochlear fissure especially vary from a very thin cast to a quite wide one (Fig. 10I2,4), the carotid foramen can be absent (Fig. 10I3, see also previously) the pyriform window is sometimes V-shaped (Fig. 10I4), and both extreme cases of foramina independence/coalescence are retrieved

(Fig. 10I). The main implication of this variation, as previously highlighted, is that the structures observed on the endocranial cast have here to be named according to the skull foramina identification rather than according to the structures crossing them; this especially stands for the basicochlear fissure that houses the ventral petrosal sinus.

III Unknown endocranial apertures (Fig. 11)

As a final point, an aperture is frequently retrieved in rhinolophids (Fig. 11) but we cannot identify its soft tissue correspondence, even after looking at the skull. This is retrieved laterally to the oval foramen and opens posteriorwards. It is big, being the same dimension or larger than the oval foramen. It opens in the bony wall that constitutes the posterior wall of the piriform lobe (and, more generally, of the cerebral hemisphere), above the pyriform window. Such aperture has not been reported in the literature to our knowledge, and it seems very unlikely to be a carotid foramen since it would mean that the internal carotid artery is of considerable thickness (whereas an almost opposite observation has been reported by Grosser [1901]). As it concerns a bony wall limiting a part of the brain, it could also be a cartilaginous wall of the braincase that would have fade away with preservation, as for the lateral wall of the subarcuate fossa (see 'Nervous imprints and exits' section and Schneider 1957). However, even on well-preserved skulls (i.e., with still some delicate and/or cartilaginous structures) used to virtually extract their endocast, this aperture is well-defined and does not seem to be an artifact. This aperture is not always unique, and a similar one, of varying size, is also found laterally (Fig. 11), sharing otherwise all its other properties. Pending further identification, we name them **unknown apertures**.

Conclusions

We provide here a detailed review of the available knowledge of brain macromorphology, endocranial anatomy, and global braincase angiology of bats. We confront this theoretical framework to a comparative sample of virtual endocasts representing most extant chiropteran families, and tentatively identify anatomical correspondences between the brain and its associated structures and the endocranial cast. This approach allows us for devising an illustrated practical picture of neurological and vascular structures one can expect to see on a chiropteran endocranial cast. This is intended to serve for future studies as a nomenclature for thoroughly describe bat endocasts, especially from fossil species, but also to compare endocasts of bat species using a common set of anatomical terms. This represents a first step to ultimately give a clear and accurate picture of the soft tissues evidences that can really be observed on a chiropteran endocast, a mandatory step in reconstructing and inferring bat paleobiology and evolutionary history. To achieve this, further works comparing soft tissues anatomy and their corresponding bony imprints are needed. Here, we intend to ease and prepare this kind of work by reviewing the previously available literature review and proposing a first, practical, comparative framework. This study also calls for others in other mammalian groups: bony imprints assessments have only been studied in hominids so far, a family that cannot serve as applicable example for mammals, and even not for primates. By repeating such kind of work in other mammalian orders, or suborders, mammalian paleoneurology would be able to more vigorously assess the numerous paleobiological and evolutionary inferences previously proposed. But beyond that field, paleontology and comparative neurobiology would eventually start to recouple.

Acknowledgements

We thank the collection curators (E. Gilissen for Africa Museum; J.-M. Pons for MNHN) for giving access to specimens and authorization to digitize them, as well as Shi et al. (2018) for giving access to such an amount of bat skulls µCT-scan through an open access repository. We also thank N. Brualla for the µCT-scanning of *Hipposideros armiger* skull during his master's internship. Finally, we thank the French ministry of higher education, research and innovation for funding the PhD thesis of one of the authors (J.M.) this work was part of. We are grateful to the MRI platform member of the national infrastructure France-BioImaging supported by the French National Research Agency (ANR-10-INBS-04, «Investments for the future»), the labex CEMEB (ANR-10-LABX-0004) and NUMEV (ANR-10-LABX-0020). This is ISEM publication 2023-XXX.

References

Almeida FC, Giannini NP, Simmons NB. 2016. The Evolutionary History of the African Fruit Bats (Chiroptera: Pteropodidae). Acta Chiropterologica 18:73–90.

Almeida FC, Simmons NB, Giannini NP. 2020. A Species-Level Phylogeny of Old World Fruit Bats with a New Higher-Level Classification of the Family Pteropodidae. Am Museum Novit 2020:1–24.

Amador LI, Moyers Arévalo RL, Almeida FC, Catalano SA, Giannini NP. 2018. Bat Systematics in the Light of Unconstrained Analyses of a Comprehensive Molecular Supermatrix. J Mamm Evol 25:37–70.

Anderson R, Maga AM. 2015. A Novel Procedure for Rapid Imaging of Adult Mouse Brains with MicroCT Using Iodine-Based Contrast. PLoS One 10:e0142974.

Anderson SC, Ruxton GD. 2020. The evolution of flight in bats: a novel hypothesis. Mamm Rev 50:426–439.

Balanoff AM, Bever GS. 2017. 1.10 The Role of Endocasts in the Study of Brain Evolution. In: Kaas JH, editor. Evolution of Nervous Systems, 2nd ed. Oxford: Academic Press, p 223–241.

Barghoorn SF. 1977. New material of Vespertiliavus Schlosser (Mammalia, Chiroptera) and suggested relationships of emballonurid bats based on cranial morphology. Am Museum Novit 2618:1–29.

Baron G, Stephan H, Frahm HD, editors. 1996. Comparative Neurobiology in Chiroptera. Basel: Birkhäuser Verlag.

Barone R, editor. 2011. Anatomie Comparée Des Mammifères Domestiques - Tome 5

Angiologie. 2nd ed. Paris: Vigot.

Barone R, Bortolami R, editors. 2004. Anatomie Comparée Des Mammifères Domestiques : Tome 6, Neurologie I, Système Nerveux Central. Paris: Vigot.

Barron DH. 1950. An experimental analysis of some factors involved in the development of the fissure pattern of the cerebral cortex. J Exp Zool 113:553–581.

Benoit J. 2015. A new method of estimating brain mass through cranial capacity in extinct proboscideans to account for the non-neural tissues surrounding their brain. J Vertebr Paleontol 35:e991021.

Bhatnagar KP. 2008. The brain of the common vampire bat, Desmodus rotundus murinus (Wagner, 1840): a cytoarchitectural atlas. Brazilian J Biol 68:583–599.

Bisconti M, Damarco P, Tartarelli G, Pavia M, Carnevale G. 2021. A natural endocast of an early Miocene odontocete and its implications in cetacean brain evolution. J Comp Neurol 529:1198–1227.

Boyer DM, Gunnell GF, Kaufman S, McGeary TM. 2017. Morphosource: Archiving and Sharing 3-D Digital Specimen Data. Paleontol Soc Pap 22:157–181.

Brown EE, Cashmore DD, Simmons NB, Butler RJ. 2019. Quantifying the completeness of the bat fossil record. Palaeontology 62:757–776.

Buchanan GD, Arata AA. 1969. Cranial vasculature of a neotropical fruit-eating bat, Artibeus lituratus. Anat Anz 124:314–325.

Burgin CJ, Colella JP, Kahn PL, Upham NS. 2018. How many species of mammals are there? J Mammal 99:1–14.

Butler PM. 1948. On the Evolution of the Skull and Teeth in the Erinaceidae, with Special

Reference to Fossil Material in the British Museum. Proc Zool Soc London 118:446–500.

Cartmill M, MacPhee RDE. 1980. Tupaiid Affinities: The Evidence of the Carotid Arteries and Cranial Skeleton. In: Luckett WP, editor. Comparative Biology and Evolutionary Relationships of Tree Shrews, Boston, MA: Springer, p 95–132.

Cheung N, McNab AA. 2003. Venous anatomy of the orbit. Investig Ophthalmol Vis Sci 44:988–995.

Cleland TA, Linster C. 2019. Central olfactory structures. Handb Clin Neurol 164:79–96.

Costidis A, Rommel SA. 2012. Vascularization of air sinuses and fat bodies in the head of the Bottlenose dolphin (Tursiops truncatus): Morphological implications on physiology. Front Physiol 3 JUL:1–23.

Cunningham JA, Rahman IA, Lautenschlager S, Rayfield EJ, Donoghue PCJ. 2014. A virtual world of paleontology. Trends Ecol Evol 29:347–357.

Dechaseaux C. 1956. L'encéphale des mammifères volants. Colloq Int du Cent Natl la Rech Sci 80:51–58.

Dechaseaux C. 1962. Cerveaux d'animaux Disparus. Paris: Masson et Cie.

Dechaseaux C. 1970. Récents résultats en paléoneurologie. Bull Académie Société Lorraines des Sci 9:223–232.

Dechaseaux C. 1973. Essais de paléoneurologie. Ann Paléontologie 59:8–132.

Dechmann DKN, Safi K. 2009. Comparative studies of brain evolution: A critical insight from the Chiroptera. Biol Rev 84:161–172.

Diamond MK. 1991. Homologies of the stapedial artery in humans, with a reconstruction of the primitive stapedial artery configuration of euprimates. Am J Phys Anthropol 84:433–

462.

Diamond MK. 1992. Homology and evolution of the orbitotemporal venous sinuses of humans. Am J Phys Anthropol 88:211–244.

Dow RS. 1942. The Evolution and Anatomy of the Cerebellum. Biol Rev 17:179–220.

Edinger T. 1926. Fossile Fledermausgehirne. Senckenbergiana 8:1–6.

Edinger T. 1929. Die fossilen Gehirne. Ergeb Anat Entwicklungsgesch 28:1–249.

Edinger T. 1949. Paleoneurology vs comparative brain anatomy. Confin Neurol 9:5–24.

Edinger T. 1961. Fossil brains reflect specialized behavior. World Neurol 2:934–41.

Edinger T. 1964a. Recent Advances in Paleoneurology. Prog Brain Res 6:147–160.

Edinger T. 1964b. Midbrain Exposure and Overlap in Mammals. Am Zool 4:5–19.

Evans HE, Lahunta A de, editors. 2012. Miller's Anatomy of the Dog. 4th ed. St. Louis, Missouri: Elsevier Saunders.

Ferreira JD, Dozo MT, Moura Bubadué J de, Kerber L. 2022. Morphology and postnatal ontogeny of the cranial endocast and paranasal sinuses of capybara (Hydrochoerus hydrochaeris), the largest living rodent. J Morphol 283:66–90.

Garcia KE, Kroenke CD, Bayly P V. 2018. Mechanics of cortical folding: stress, growth and stability. Philos Trans R Soc London B, Biol Sci 373:20170321.

Giannini NP, Wible JR, Simmons NB. 2006. On the Cranial Osteology of Chiroptera. I. Pteropus (Megachiroptera: Pteropodidae). Bull Am Museum Nat Hist 2006:1–134.

Gignac PM, Kley NJ, Clarke JA, Colbert MW, Morhardt AC, Cerio D, Cost IN, Cox PG, Daza JD, Early CM, Echols MS, Henkelman RM, et al. 2016. Diffusible iodine-based contrast-enhanced computed tomography (diceCT): an emerging tool for rapid,

high-resolution, 3-D imaging of metazoan soft tissues. J Anat 228:889–909.

Grosser O. 1901. Zur Anatomie und Entwickelungsgeschichte des Gefässsystemes der Chiropteren. Anat Hefte 17:203–424.

Hackethal H. 1981. Die bedeutung hirnmorphologischer Merkmale für die taxonomie der placentalen säuger. Mitteilungen aus dem Museum für Naturkd Berlin Zool Museum und Inst für Spez Zool 57:233–340.

Hand SJ. 1997. New Miocene leaf-nosed bats (Microchiroptera: Hipposideridae) from Riversleigh, northwestern Queensland. Mem Queensl Museum 41:335–349.

Hassanin A, Bonillo C, Tshikung D, Pongombo Shongo C, Pourrut X, Kadjo B, Nakouné E, Tu VT, Prié V, Goodman SM. 2020. Phylogeny of African fruit bats (Chiroptera, Pteropodidae) based on complete mitochondrial genomes. J Zool Syst Evol Res 58:1395–1410.

Hedrick BP, Yohe L, Linden A Vander, Dávalos LM, Sears K, Sadier A, Rossiter SJ, Davies KTJ, Dumont ER. 2018. Assessing Soft-Tissue Shrinkage Estimates in Museum Specimens Imaged With Diffusible Iodine-Based Contrast-Enhanced Computed Tomography (diceCT). Microsc Microanal 24:284–291.

Hegedus SA, Shackelford RT. 1965. A comparative-anatomical study of the craniocervical venous systems in mammals, with special reference to the dog: Relationship of anatomy to measurements of cerebral blood flow. Am J Anat 116:375–386.

Henson OWJ. 1970. 2 The Central Nervous System. In: Wimsatt WA, editor. Biology of Bats: Volume 2, New York, NY: Academic Press, p 57.

Hitier M, Zhang M, Labrousse M, Barbier C, Patron V, Moreau S. 2013. Persistent stapedial arteries in human: From phylogeny to surgical consequences. Surg Radiol Anat 35:883–891.

Hutcheon JM, Kirsch JAW, Garland Jr T. 2002. A Comparative Analysis of Brain Size in Relation to Foraging Ecology and Phylogeny in the Chiroptera. Brain Behav Evol 60:165–180.

Jerison HJ. 1990a. Fossil Brains and the Evolution of the Neocortex. In: Finlay BL, Innocenti G, Scheich H, editors. The Neocortex, Boston, MA: Springer US, p 5–19.

Jerison HJ. 1990b. Fossil Evidence on the Evolution of the Neocortex. In: Jones EG, Peters A, editors. Comparative Structure and Evolution of Cerebral Cortex, Part I, New York: Springer Science and Business Media LLC, p 285–309.

Jolicoeur P, Pirlot P, Baron G, Stephan H. 1984. Brain Structure and Correlation Patterns in Insectivora, Chiroptera, and Primates. Syst Biol 33:14–29.

Kallen FC. 1977. The cardiovascular system of bats: Structure and function. In: Wimsatt WA, editor. Biology of Bats: Volume 3, New York, NY: Academic Press, p 289–483.

Kochetkova VI. 1978. The subject matter of paleoneurological studies. In: Kochetkova VI, Jerison HJ, Jerison I, editors. Paleoneurology, Washington, D.C.: V. H. Winston & Sons, p 17–45.

Larsell O, Dow RS. 1935. The development of the cerebellum in the bat (Corynorhinus sp.) and certain other mammals. J Comp Neurol 62:443–468.

Lebrun R. 2018. MorphoDig, an open-source 3D freeware dedicated to biology.

Lyras GA. 2009. The evolution of the brain in Canidae (Mammalia: Carnivora). Scr Geol 1–93.

Mann G. 1961. Bulbus olfactorius accessorius in chiroptera. J Comp Neurol 116:135–144.

Martínez G, Dozo MT, Vera B, Cerdeño E. 2019. Paleoneurology, auditory region, and associated soft tissue inference in the late Oligocene notoungulates Mendozahippus

fierensis and Gualta cuyana (Toxodontia) from central-western Argentina. J Vertebr Paleontol 39:1–19.

Maugoust J. 2021. Evolution des structures endocrâniennes des Chiroptera (Mammalia), apports des formes fossiles. Université de Montpellier, unpublished PhD thesis.

Maugoust J, Orliac MJ. 2021. Endocranial Cast Anatomy of the Extinct Hipposiderid Bats Palaeophyllophora and Hipposideros (Pseudorhinolophus) (Mammalia: Chiroptera). J Mamm Evol 28:679–706.

McDaniel VR. 1976. Brain Anatomy. In: Baker RJ, Knox Jones Jr. J, Carter DC, editors. Biology of Bats of the New World Family Phyllostomidae. Part I, Lubbock, Texas: Texas Tech Press, p 147–200.

Muizon de C, Billet G, Argot C, Ladevèze S, Goussard F. 2015. Alcidedorbignya inopinata, a basal pantodont (Placentalia, Mammalia) from the early Palaeocene of Bolivia: Anatomy, phylogeny and palaeobiology. Geodiversitas 37:397–631.

Mutuş R. 2001. Macroanatomical and Morphometric Investigation on the Maxillary Vein in Rabbits. Turkish J Vet Anim Sci 25:803–809.

NAV NAV. 2017. International Committee on Veterinary Gross Anatomical Nomenclature (I.C.V.G.A.N.). 6th ed. Hanover (Germany), Ghent (Belgium), Columbia, MO (USA), Rio de Janeiro (Brazil): The Editorial Committee with permission of the World Association of Veterinary Anatomists (W.A.V.A.).

Neuweiler G. 2000. Central nervous system. In: Neuweiler G, editor. The Biology of Bats, New York: Oxford University Press, p 117–139.

Norberg UML, Rayner J. 1987. Ecological morphology and flight in bats (Mammalia; Chiroptera): wing adaptations, flight performance, foraging strategy and echolocation. Philos

Trans R Soc London B, Biol Sci 316:335–427.

Orliac MJ, O'Leary MA. 2016. The inner ear of Protungulatum (Pan-Euungulata, Mammalia). J Mamm Evol 23:337–352.

Orlov YA, editor. 1961. В Мире Древних Животных (In the Ancient Animal Kingdom). Moscow: Publishing House of the Academy of Sciences of the USSR.

Palermo EC. 2013. Anatomy of the periorbital region. Surg Cosmet Dermatol 5:245–256.

Pfaff C, Schultz JA, Schellhorn R. 2018. The vertebrate middle and inner ear: A short overview.

Pigache RM. 1970. The Anatomy of "Paleocortex." Berlin, Heidelberg: Springer-Verlag.

Radtke-Schuller S, Fenzl T, Peremans H, Schuller G, Firzlaff U. 2020. Cyto- and myeloarchitectural brain atlas of the pale spear-nosed bat (Phyllostomus discolor) in CT Aided Stereotaxic Coordinates. Brain Struct Funct 225:2509–2520.

Raghavan R, Lawton W, Ranjan SR, Viswanathan RR. 1997. A continuum mechanics-based model for cortical growth. J Theor Biol 187:285–296.

Ravel A, Orliac MJ. 2015. The inner ear morphology of the 'condylarthran' Hyopsodus lepidus. Hist Biol 27:957–969.

Reinhard KR, Miller ME, Evans HE. 1962. The craniovertebral veins and sinuses of the dog. Am J Anat 111:67–87.

Revilliod P. 1920. Contribution à l'étude des Chiroptères des terrains tertiaires (2ème partie). Mémoires la Société Paléontologique Suisse 44:61–130.

Robertson A, editor. 1828. Conversations on Anatomy, Physiology, and Surgery. Volume 2. Philadelphia: Towar & Hogan.

Robson S, Ludtke JA, Theodor JM. 2022. Petrosal and Basicranial Morphology of Leptoreodon major (Protoceratidae, Artiodactyla). Vertebr Anat Morphol Palaeontol 9:116–130.

Safi K, Seid MA, Dechmann DKN. 2005. Bigger is not always better: when brains get smaller. Biol Lett 1:283–286.

Scalia F, Rasweiler IV JJ, Scalia J, Orman R, Stewart M, editors. 2013. Forebrain Atlas of the Short-Tailed Fruit Bat, Carollia Perspicillata. New York, NY: Springer New York.

Schneider R. 1957. Morphologische Untersuchungen am Gehirn der Chiroptera (Mammalia). Abhandlungen der Senckenbergischen Naturforschenden Gesellschaft 495:1–92.

Schneider R. 1966. Das Gehirn von Rousettus Aegyptiacus (E. GEOFFROY 1810) (Megachiroptera, Chiroptera, Mammalia). Ein mit Hilfe mehrerer Schnittserien erstellter Atlas. Abhandlungen der Senckenbergischen Naturforschenden Gesellschaft 513:1–160.

Scremin OU. 2015. Cerebral Vascular System. 4th ed. London: Elsevier.

Shi JJ, Rabosky DL. 2015. Speciation dynamics during the global radiation of extant bats. Evolution (N Y) 69:1528–1545.

Shi JJ, Westeen EP, Rabosky DL. 2018. Digitizing extant bat diversity : An open-access repository of 3D μ CT-scanned skulls for research and education. PLoS One 13:1–13.

Smith GE. 1902a. On the Homologies of the Cerebral Sulci. J Anat Physiol 36:309–319.

Smith GE. 1902b. The Primary Subdivision of the Mammalian Cerebellum. J Anat Physiol 36:381–5.

Smith GE. 1903. On the Morphology of the Brain in the Mammalia, with Special

Reference to that of the Lemurs, Recent and Extinct. Trans Linn Soc London 2nd Ser Zool 8:319–432.

Spoor F, Wood B, Zonneveld F. 1994. Implications of early hominid labyrinthine morphology for evolution of human bipedal locomotion. Nature 369:645–648.

Standring S, editor. 2016. Gray's Anatomy. 41th ed. London: Elsevier Health Sciences.

Stephan H, Pirlot P. 1970. Volumetric Comparisons of Brain Structures in Bats. J Zool Syst Evol Res 8:200–236.

Tandler J. 1899. Zur vergleichenden Anatomie der Kopfarterien bei den Mammalia. Denkschriften der Kais Akad der Wissenschaften, Math Klasse 67:677–784.

Tandler J. 1901. Zur vergleichenden Anatomie der Kopfarterien bei den Mammalia. Anat Hefte 18:328–368.

Teeling EC, Jones G, Rossiter SJ. 2016. Phylogeny, Genes, and Hearing: Implications for the Evolution of Echolocation in Bats. In: Fenton MB, Grinnell AD, Popper AN, Fay RR, editors. Bat Bioacoustics, New York, NY: Springer New York, p 25–54.

Voogd J, Nieuwenhuys R, Dongen PAM van, Donkelaar HJ ten. 1998. Mammals. In: Nieuwenhuys R, Donkelaar HJ ten, Nicholson C, editors. The Central Nervous System of Vertebrates, Berlin, Heidelberg: Springer Berlin Heidelberg, p 1637–2097.

Washington SD, Hamaide J, Jeurissen B, Steenkiste G van, Huysmans T, Sijbers J, Deleye S, Kanwal JS, Groof G De, Liang S, Audekerke J Van, Wenstrup JJ, et al. 2018. A three-dimensional digital neurological atlas of the mustached bat (Pteronotus parnellii). Neuroimage 183:300–313.

Welker W. 1990. Why Does Cerebral Cortex Fissure and Fold? In: Jones EG, Peters A,

editors. Cerebral Cortex: Volume 8B: Comparative Structure and Evolution of Cerebral Cortex, Part 2, New York: Plenum Press, p 3–136.

Wible JR. 1984. The ontogeny and phylogeny of the mammalian cranial arterial pattern. Duke University, unpublished PhD thesis.

Wible JR. 1987. The eutherian stapedial artery: character analysis and implications for superordinal relationships. Zool J Linn Soc 91:107–135.

Wible JR. 1993. Cranial circulation and relationships of the Colugo Cynocephalus (Dermoptera, Mammalia). Am Museum Novit 3072:27.

Wible JR. 2010. Petrosal anatomy of the nine-banded armadillo, Dasypus novemcinctus Linnaeus, 1758 (Mammalia, Xenarthra, Dasypodidae). Ann Carnegie Museum 79:1–28.

Wible JR. 2011. On the treeshrew skull (Mammalia, Placentalia, Scandentia). Ann Carnegie Museum 79:149–230.

Wible JR. 2022. Petrosal and cranial vascular system of the early Eocene palaeoryctid mammal Eoryctes melanus from northwestern Wyoming, USA. Acta Palaeontol Pol 67:203–220.

Wible JR, Davis DL. 2000. Ontogeny of the chiropteran basicranium, with reference to the Indian false vampire bat, Megaderma lyra. In: Adams RA, Pedersen SC, editors. Ontogeny, Functional Ecology, and Evolution of Bats, New York: Cambridge University Press, p 214–246.

Wible JR, Zeller U. 1994. Cranial circulation of the pen-tailed tree shrew Ptilocercus lowii and relationships of Scandentia. J Mamm Evol 2:209–230.

Wilson LAB, Hand SJ, López-Aguirre C, Archer M, Black KH, Beck RMD, Armstrong KN,

Wroe S. 2016. Cranial shape variation and phylogenetic relationships of extinct and extant Old World leaf-nosed bats. Alcheringa 40:509–524.

Yao L, Brown J-P, Stampanoni M, Marone F, Isler K, Martin RD. 2012. Evolutionary Change in the Brain Size of Bats. Brain Behav Evol 80:15–25.

Figures and table captions

Figure 1: virtual endocranial casts of the sample used here showing noctilionoids (A- *Thyroptera tricolor*, Thyropteridae; B- *Noctilio albiventris*, Noctilionidae; C- *Mormoops blainvilli*, Mormoopidae; D- *Macrotus waterhousii*, Phyllostomidae) and vespertilionoids (E- *Nyctiellus lepidus*, Natalidae; F- *Cheiromeles torquatus*, Molossidae; G- *Miniopterus schreibersii*, Miniopteridae; H- *Kerivoula pellucida*, Vespertilionidae; I- *Scotophilus kuhlii*, Vespertilionidae), each in dorsal (top left), ventral (bottom left), lateral right (top right), and lateral left views (bottom right). Scale bar of 1cm for each specimen

Figure 2: virtual endocranial casts of the sample used here showing emballonuroids (A- *Balantiopteryx plicata*, Emballonuridae; B- *Nycteris macrotis*, Nycteridae), rhinolophoids (C- *Rhinolophus luctus*, Rhinolophidae; D- *Triaenops persicus*, Rhinonycteridae; E- *Hipposideros armiger*, Hipposideridae; F- *Lavia frons*, Megadermatidae; G- *Rhinopoma hardwickii*, Rhinopomatidae), and pteropodids (H- *Sphaerias blanfordi*; I- *Rousettus aegyptiacus*; J- *Pteropus pumilus*), each in dorsal (top left), ventral (bottom left), lateral right (top right), and lateral left views (bottom right). Scale bar of 1cm for each specimen

Figure 3: simplified scheme of the structures found on a chiropteran endocranial cast, excepting the neopallial sulci (see Fig. 5A-F) in dorsal (a), ventral (b) and lateral (c) views. See abbreviations in Material & Methods section

Figure 4: brain parts visible on an endocranial cast. A- telencephalic components. B- importance of the dorsum sellae for locating the “real” hypophysis cast. C- cerebellar components. D- variation in the delineation of the hypophysis cast (not visible-D1, blurry outline-D2, clear outline-D3). E- variable exposure of the mesencephalic tectum (all four colliculi clearly delineated-E1, rostral colliculi barely delineated-E2, only caudal colliculi

delineated-E3, caudal colliculi partly hidden-E4, whole tectum covered in a microchiropteran-E5, whole tectum covered in a megachiropteran-E6). F- various subdivisions of the cerebellar lobules. G- area where the flocculus ('F') should be seen. H- parafloccular apertures. I- pons-medulla oblongata continuum

Figure 5: neopallial sulci visible on an endocranial cast. A- theoretical neopallial complexification pattern (A1: case with a single sylvian sulcus, separating the temporal area from the fronto-orbito-parieto-occipital (FOPO) area, with a putative insular area in the anteroventral continuation of the temporal one; A2: case with an orbital sulcus separating the fronto-orbital cortex anteriorly from the other areas posteriorly, with two transitional areas between that area and the parietal and insular areas respectively; A3 to A6: cases of increasing complexity of the sylvian area, with appearance of a bridge sulcus in A3, its posterior bending in A4, the appearance of a lateral sulcus in A5, and the complex configuration of the sylvio-lateral area in A6 with up to three bridge and supralateral sulci), the colors of neopallial areas indicating the cortices (green- fronto-orbital; orange- parietal; brown- occipital; light blue- insular; blue- temporal) and the color gradient areas indicating a putative transitional area. B- sylvian sulcus. C- supralateral sulcus (C1) or sulci (C2). D- variation in orientation, shape, and number of the bridge sulcus/sulci (D1- single, straight, antero-dorsally pointing; D2-single, somewhat curved, dorsally pointing; D3-multiple). E- infrasylvian sulcus. F- orbital sulcus. G- intermediate sulcus

Figure 6: cerebellar foldings and imprints visible on an endocranial cast. A- paramedian fissure (A1- wide and shallow, A2- thin and deep). B- lateral expansion of the uvula (lobule IX). C- ventral parafloccular fossa. D- imprint of the lateral semicircular canal. E- lateral parafloccular sulcus

Figure 7: braincase openings for (among others) cranial nerves. A- all nerve exits. B- imprint of the trigeminal ganglion. C- variation in the coalescence between optic foramina and sphenorbital fissures (C1- no coalescence, distant openings, C2- no coalescence, close openings, C3- moderate coalescence, optic foramina still partly decipherable, C4- advanced coalescence). D- sphenorbital fissure subdivision. E- distinction between caudal alisphenoid canal foramen and anterior opening of the pterygoid canal

Figure 8: theoretical pattern of main arteries (8A) and veins (8B) crossing the braincase. Hashed lines indicate inter-specific variation. Dotted lines indicate potential absence. Megachiropteran-only features indicated in pink (arteries) and purple (veins). “Microchiropteran”-only featues indicated in yellow (arteries) and sky blue (veins)

Figure 9: braincase openings and imprints for (among others) arterial structures. A- supracribriform aperture. B- entrance of superior ramus trunk cast. C- superior ramus trunk and its anterior branch casts. D- anterior branch of superior ramus cast absence (D1) or presence (D2-D3) and shape (D2- sigmoid, D3-convex). E- density of meningeal rami casts arising from the anterior branch of superior ramus. F- anterior continuation (F1) or not (F2) of the anterior branch of superior ramus cast in megachiropterans. G- caudal alisphenoid canal foramen independence (G1- megachiropteran, G2- “microchiropteran) or coalescence with oval foramen (G3- megachiropteran, G4-“microchiropteran”). H- internal carotid artery entrance in the braincase (H1-H3) or not (H4), through a carotid foramen (H2-H3) or a carotid canal with an endocranial carotid foramen (H1), leaving a carotid sulcus (H1-H2) or not (H3). I- carotid canal, with associated endocranial carotid foramen located either far from piriform lobe posterior wall (I1) or within it and close to oval foramen (I2). J- middle cerebral artery cast. K- connecting vessel cast

Figure 10: braincase openings and imprints for (among others) venous structures. A- dorsal sagittal and rostral transverse sinuses casts. B- rostral transverse sinus apertures being unique (B1) or multiple (B2). C- sphenorbital emissary vein foramen with cases of confluent optic foramen with sphenorbital fissure (C1) or not (C2). D- dorsal sagittal and transverse sinuses casts. E- pathway of transverse sinus cast relative to mesencephalic colliculi. F- dorsal cerebellar vein cast. G- communicant aperture and its relationships with surrounding vessel casts, with cases without (G1) or with (G2-G4) superior ramus trunk cast, showing the nature of the aperture above (G3) and below (G4) the superior ramus trunk cast. H- lateral continuity between cerebellar hemisphere and sigmoid sinus. I- presence/absence and independence/coalescence of apertures surrounding the petrosal cast (I1- all four apertures independent, I2- all apertures independent but no basicochlear fissure, I3- all apertures independent but no carotid foramen, I4- all apertures coalescent with probable basicochlear fissure)

Figure 11: unknown apertures, also highlighting the difference in their number and shape between both sides

Table 1: Information regarding institution, taxonomy, scanning parameters, and segmentation parameters of the comparative sample used here. Institution abbreviations: UMMZ- University of Michigan, Museum of Zoology, Ann Arbor, USA; AMNH- American Museum of National History, New York, USA; AM- Africa Museum, Tervuren, Belgium; UM- University of Montpellier, Montpellier, France; MNHN- Muséum National d'Histoire Naturelle, Paris, France

Institution	Taxonomy		Scanning			Segmentation
Museum	Number	Binom	Voltage (kV)	Frames/second	Intensity (µA)	Used voxel size (µm)
UMMZ	102659	Balantiopteryx plicata	70	4	114	20
AMNH	M-187705	Nycteris macrotis	70	4	114	20
UMMZ	53240	Thyroptera tricolor	70	4	114	20
UMMZ	105827	Noctilio albiventris	70	4	114	20
AMNH	M-271513	Mormoops blainvilli	70	4	114	20
UMMZ	95718	Macrotus waterhousii	70	4	114	20
UMMZ	105767	Nyctiellus lepidus	70	4	114	20
AMNH	M-247585	Cheiromeles torquatus	70	4	114	40
UMMZ	156998	Miniopterus schreibersii	70	4	114	20
UMMZ	161396	Kerivoula pellucida	70	4	114	20
UMMZ	157013	Scotophilus kuhlii	70	4	114	20
MNHN	CG-2006-87	Rhinolophus luctus	70	7	142	23,82
MRAC	RG 38552	Triaenops persicus	80	6	110	35,72
UM	CHI 762 V	Hipposideros armiger	59	-	167	18,08
MRAC	RG 12268	Lavia frons	80	4,5	125	23,82
MRAC	RG M31166	Rhinopoma hardwickei	80	6	110	35,72
AMNH	M-274330	Sphaerias blanfordi	70	4	114	40
UMMZ	161026	Rousettus aegyptiacus	70	4	114	40
UMMZ	162253	Pteropus pumilus	70	4	114	40

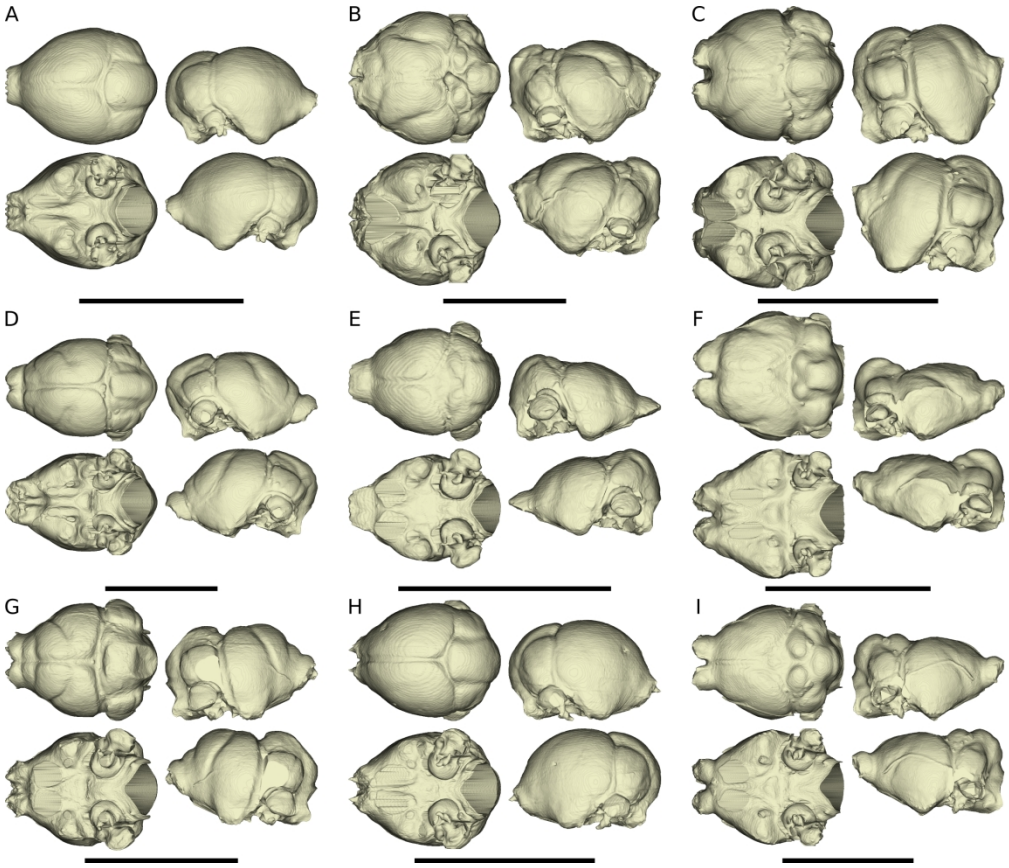

Figure 1: virtual endocranial casts of the sample used here showing noctilionoids (A- Thyroptera tricolor, Thyropteridae; B- Noctilio albiventris, Noctilionidae; C- Mormoops blainvilli, Mormoopidae; D- Macrotus waterhousii, Phyllostomidae) and vespertilionoids (E- Nyctiellus lepidus, Natalidae; F- Cheiromeles torquatus, Molossidae; G- Miniopterus schreibersii, Miniopteridae; H- Kerivoula pellucida, Vespertilionidae; I- Scotophilus kuhlii, Vespertilionidae), each in dorsal (top left), ventral (bottom left), lateral right (top right), and lateral left views (bottom right). Scale bar of 1cm for each specimen

661x566mm (96 x 96 DPI)

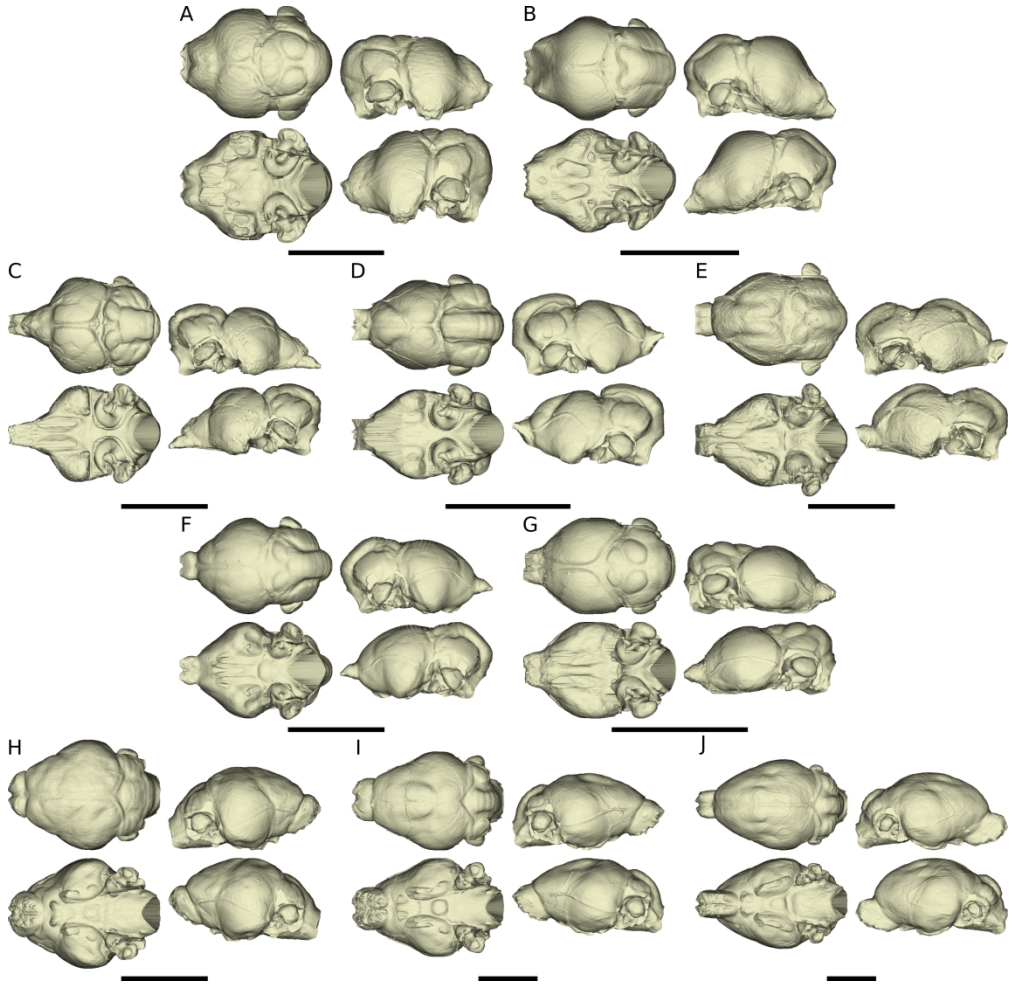

Figure 2: virtual endocranial casts of the sample used here showing emballonuroids (A- Balantiopteryx plicata, Emballonuridae; B- Nycteris macrotis, Nycteridae), rhinolophoids (C- Rhinolophus luctus, Rhinolophidae; D- Triaenops persicus, Rhinonycteridae; E- Hipposideros armiger, Hipposideridae; F- Lavia frons, Megadermatidae; G- Rhinopoma hardwickii, Rhinopomatidae), and pteropodids (H- Sphaerias blanfordi; I- Rousettus aegyptiacus; J- Pteropus pumilus), each in dorsal (top left), ventral (bottom left), lateral right (top right), and lateral left views (bottom right). Scale bar of 1cm for each specimen

661x643mm (96 x 96 DPI)

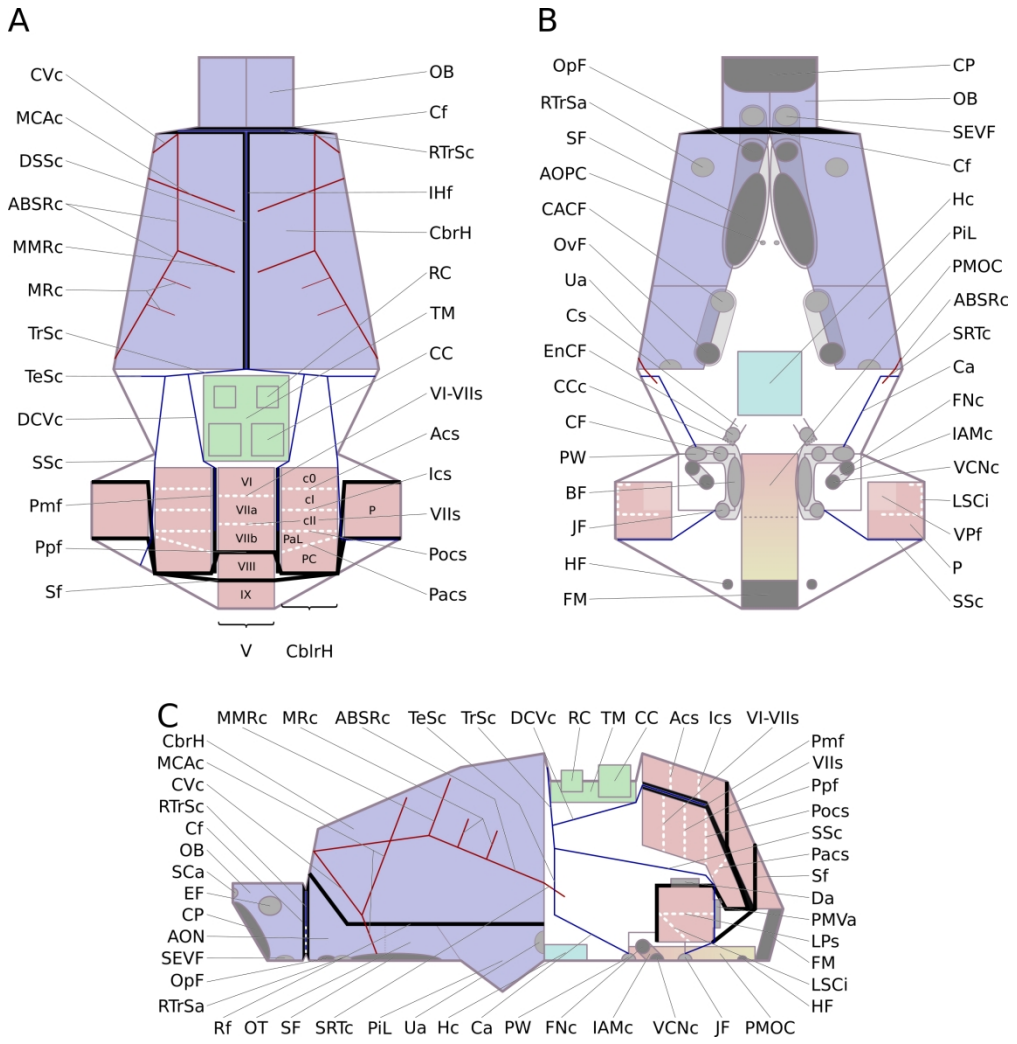

Figure 3: simplified scheme of the structures found on a chiropteran endocranial cast, excepting the neopallial sulci (see Fig. 5A-F) in dorsal (a), ventral (b) and lateral (c) views. See abbreviations in Material & Methods section

643x661mm (96 x 96 DPI)

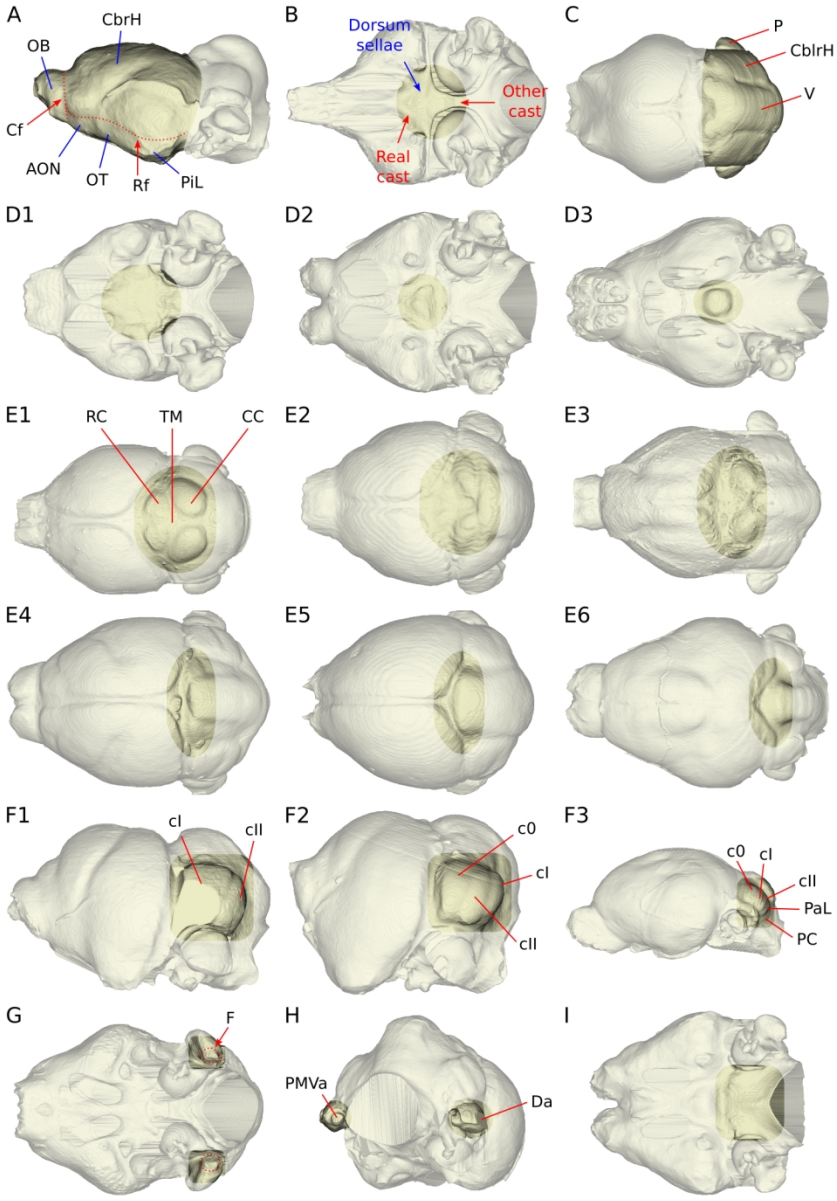

Figure 4: brain parts visible on an endocranial cast. A- telencephalic components. B- importance of the dorsum sellae for locating the "real" hypophysis cast. C- cerebellar components. D- variation in the delineation of the hypophysis cast (not visible-D1, blurry outline-D2, clear outline-D3). E- variable exposure of the mesencephalic tectum (all four colliculi clearly delineated-E1, rostral colliculi barely delineated-E2, only caudal colliculi delineated-E3, caudal colliculi partly hidden-E4, whole tectum covered in a microchiropteran-E5, whole tectum covered in a megachiropteran-E6). F- various subdivisions of the cerebellar lobules. G- area where the flocculus ('F') should be seen. H- paraflocculus apertures. I- pons-medulla oblongata continuum

396x567mm (96 x 96 DPI)

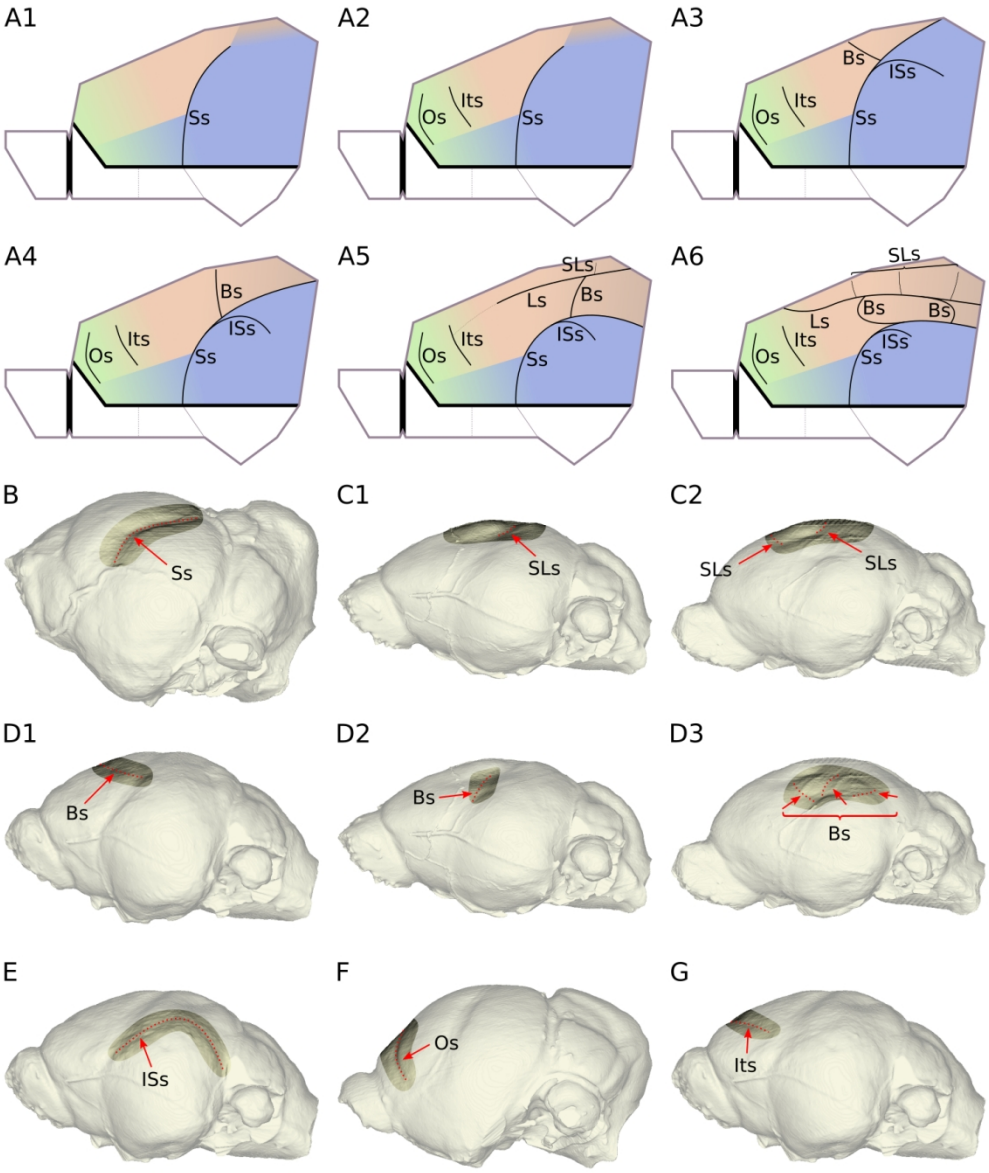

Figure 5: neopallial sulci visible on an endocranial cast. A- theoretical neopallial complexification pattern (A1: case with a single sylvian sulcus, separating the temporal area from the fronto-orbito-parieto-occipital (FOPO) area, with a putative insular area in the anteroventral continuation of the temporal one; A2: case with an orbital sulcus separating the fronto-orbital cortex anteriorly from the other areas posteriorly, with two transitional areas between that area and the parietal and insular areas respectively; A3 to A6: cases of increasing complexity of the sylvian area, with appearance of a bridge sulcus in A3, its posterior bending in A4, the appearance of a lateral sulcus in A5, and the complex configuration of the sylvio-lateral area in A6 with up to three bridge and supralateral sulci), the colors of neopallial areas indicating the cortices (green- fronto-orbital; orange- parietal; brown- occipital; light blue- insular; blue- temporal) and the color gradient areas indicating a putative transitional area. B- sylvian sulcus. C- supralateral sulcus (C1) or sulci (C2). D- variation in orientation, shape, and number of the bridge sulcus/sulci (D1- single, straight, antero-dorsally pointing; D2-single, somewhat curved, dorsally pointing; D3-multiple). E- infrasylvian sulcus. F- orbital sulcus. G- intermediate sulcus

396x472mm (96 x 96 DPI)

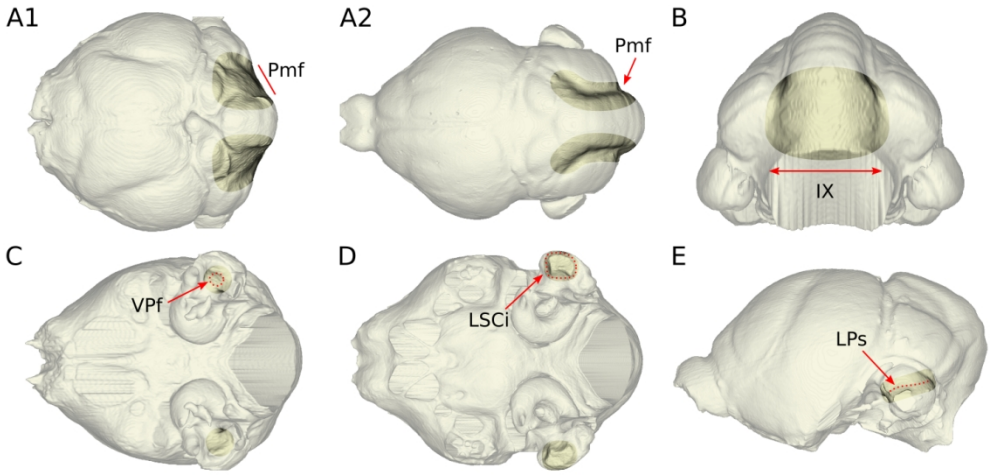

Figure 6: cerebellar foldings and imprints visible on an endocranial cast. A- paramedian fissure (A1- wide and shallow, A2- thin and deep). B- lateral expansion of the uvula (lobule IX). C- ventral paraflocular fossa. D- imprint of the lateral semicircular canal. E- lateral paraflocular sulcus

396x188mm (96 x 96 DPI)

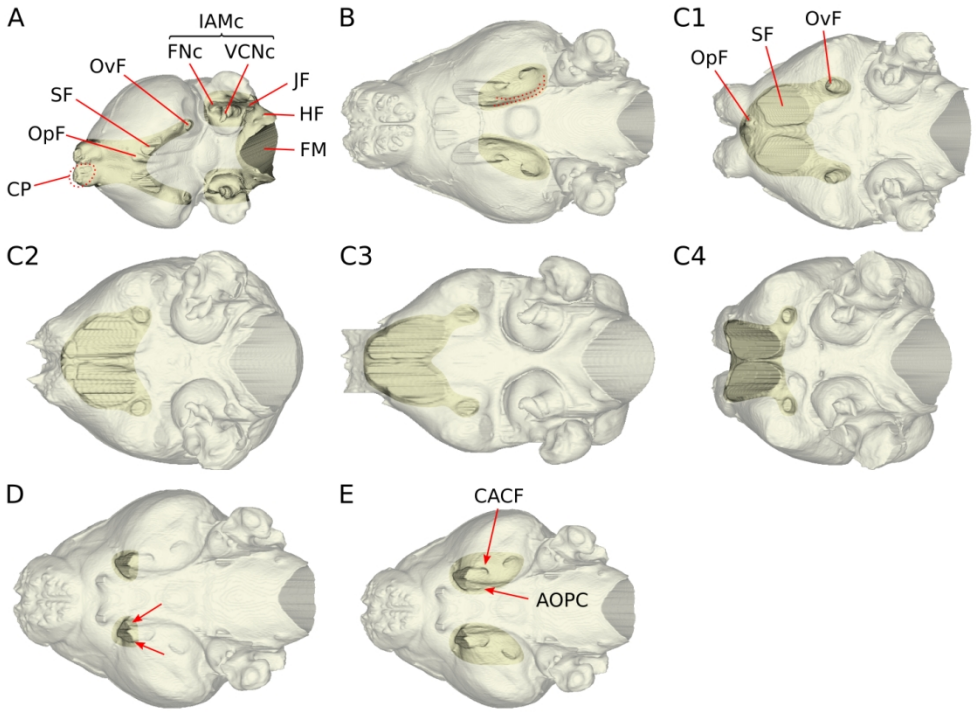

Figure 7: braincase openings for (among others) cranial nerves. A- all nerve exits. B- imprint of the trigeminal ganglion. C- variation in the coalescence between optic foramina and sphenorbital fissures (C1- no coalescence, distant openings, C2- no coalescence, close openings, C3- moderate coalescence, optic foramina still partly decipherable, C4- advanced coalescence). D- sphenorbital fissure subdivision. E- distinction between caudal alisphenoid canal foramen and anterior opening of the pterygoid canal

396x283mm (96 x 96 DPI)

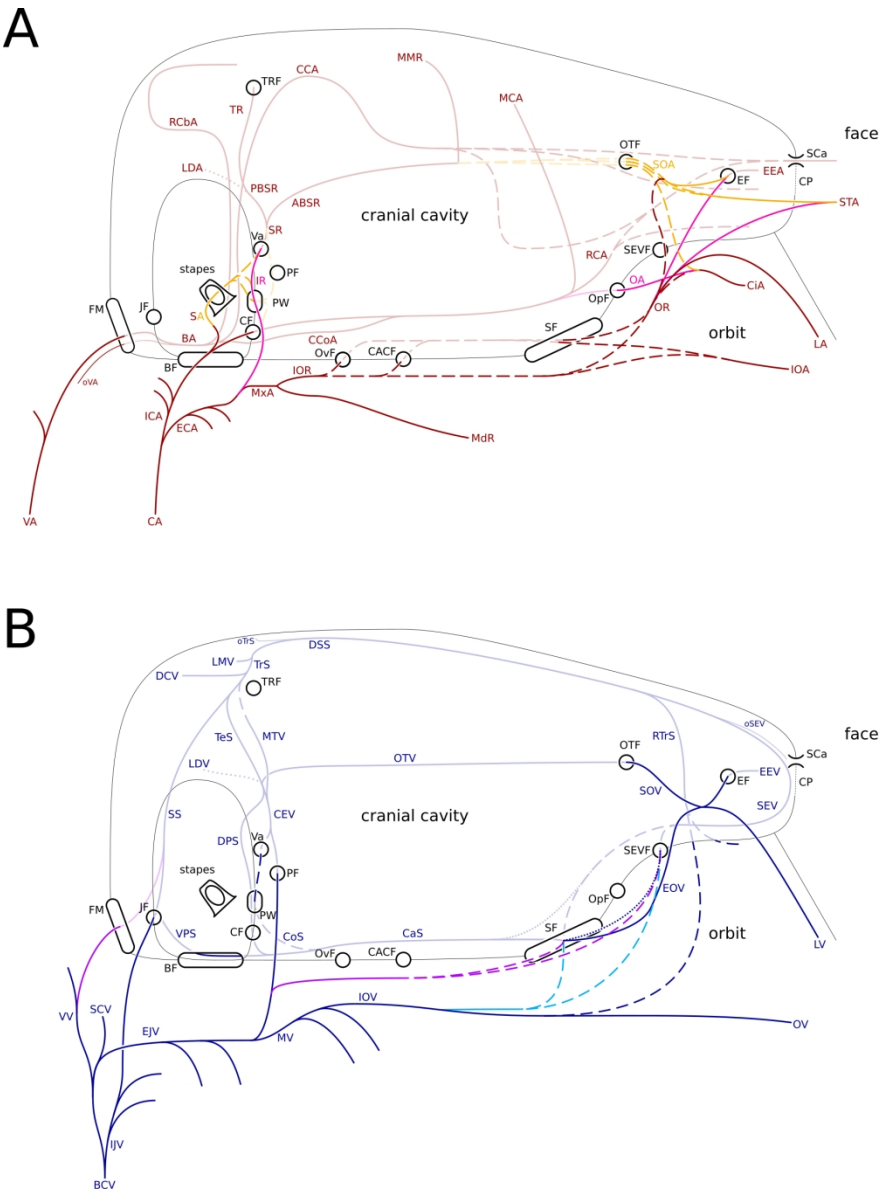

Figure 8: theoretical pattern of main arteries (8A) and veins (8B) crossing the braincase. Hashed lines indicate inter-specific variation. Dotted lines indicate potential absence. Megachiropteran-only features indicated in pink (arteries) and purple (veins). "Microchiropteran"-only featues indicated in yellow (arteries) and sky blue (veins)

483x661mm (96 x 96 DPI)

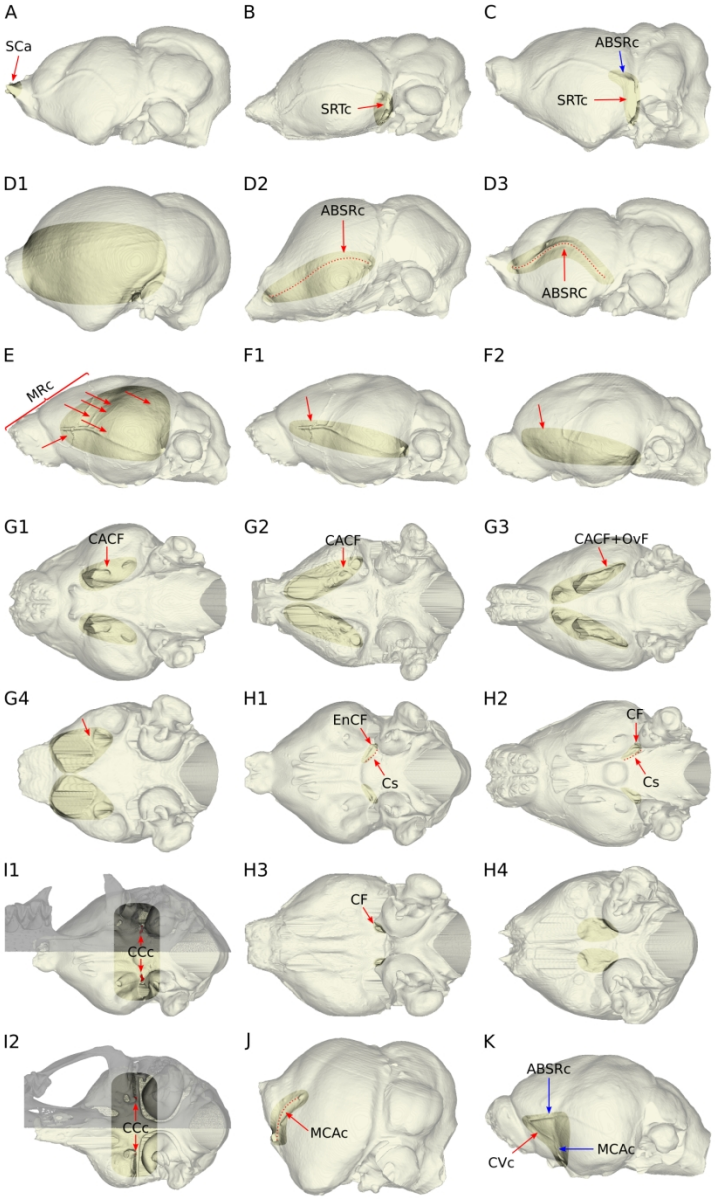

Figure 9: braincase openings and imprints for (among others) arterial structures. A- supracribriform aperture. B- entrance of superior ramus trunk cast. C- superior ramus trunk and its anterior branch casts. D- anterior branch of superior ramus cast absence (D1) or presence (D2-D3) and shape (D2- sigmoid, D3- convex). E- density of meningeal rami casts arising from the anterior branch of superior ramus. F- anterior continuation (F1) or not (F2) of the anterior branch of superior ramus cast in megachiropterans. G- caudal alisphenoid canal foramen independence (G1- megachiropteran, G2- "microchiropteran) or coalescence with oval foramen (G3- megachiropteran, G4-"microchiropteran"). H- internal carotid artery entrance in the braincase (H1-H3) or not (H4), through a carotid foramen (H2-H3) or a carotid canal with an endocranial carotid foramen (H1), leaving a carotid sulcus (H1-H2) or not (H3). I- carotid canal, with associated endocranial carotid foramen located either far from piriform lobe posterior wall (I1) or within it and close to oval foramen (I2). J- middle cerebral artery cast. K- connecting vessel cast

396x661mm (96 x 96 DPI)

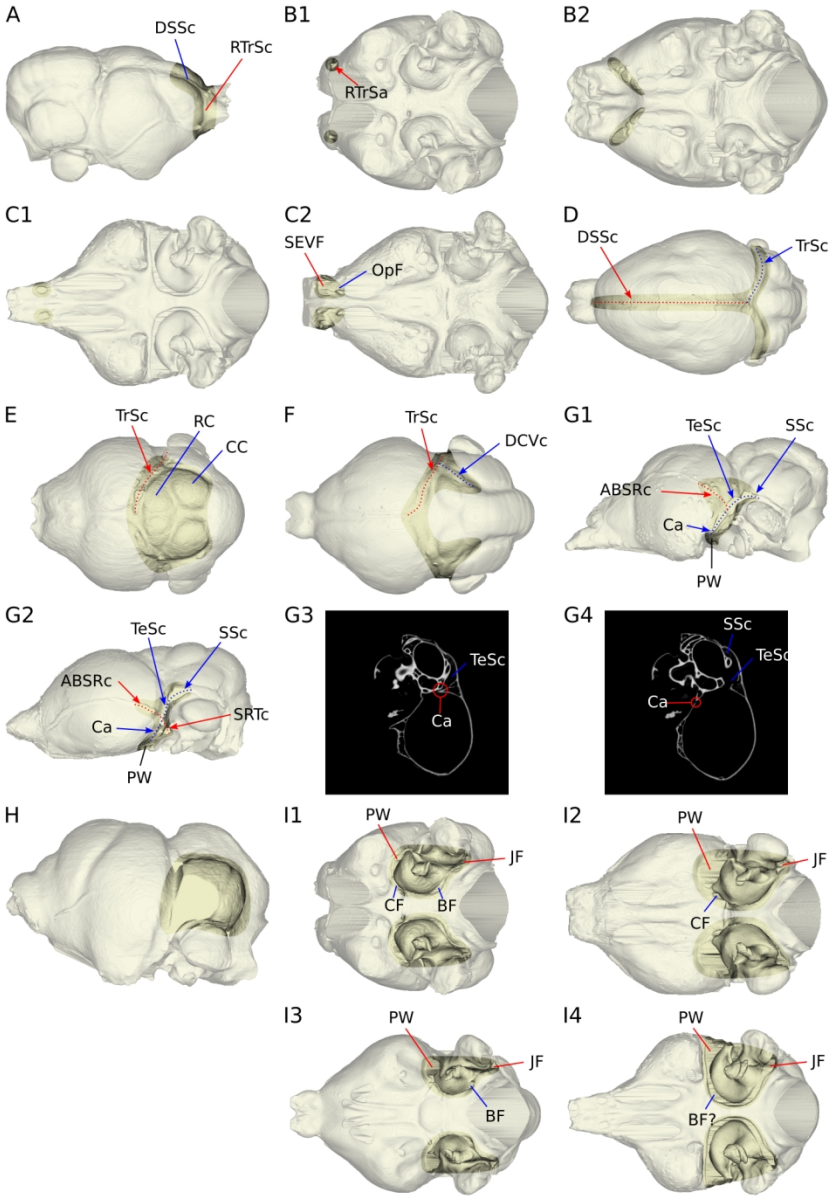

Figure 10: braincase openings and imprints for (among others) venous structures. A- dorsal sagittal and rostral transverse sinuses casts. B- rostral transverse sinus apertures being unique (B1) or multiple (B2). C- sphenorbital emissary vein foramen with cases of confluent optic foramen with sphenorbital fissure (C1) or not (C2). D- dorsal sagittal and transverse sinuses casts. E- pathway of transverse sinus cast relative to mesencephalic colliculi. F- dorsal cerebellar vein cast. G- communicant aperture and its relationships with surrounding vessel casts, with cases without (G1) or with (G2-G4) superior ramus trunk cast, showing the nature of the aperture above (G3) and below (G4) the superior ramus trunk cast. H- lateral continuity between cerebellar hemisphere and sigmoid sinus. I- presence/absence and independence/coalescence of apertures surrounding the petrosal cast (I1- all four apertures independent, I2- all apertures independent but no basicochlear fissure, I3- all apertures independent but no carotid foramen, I4- all apertures coalescent with probable basicochlear fissure)

396x567mm (96 x 96 DPI)

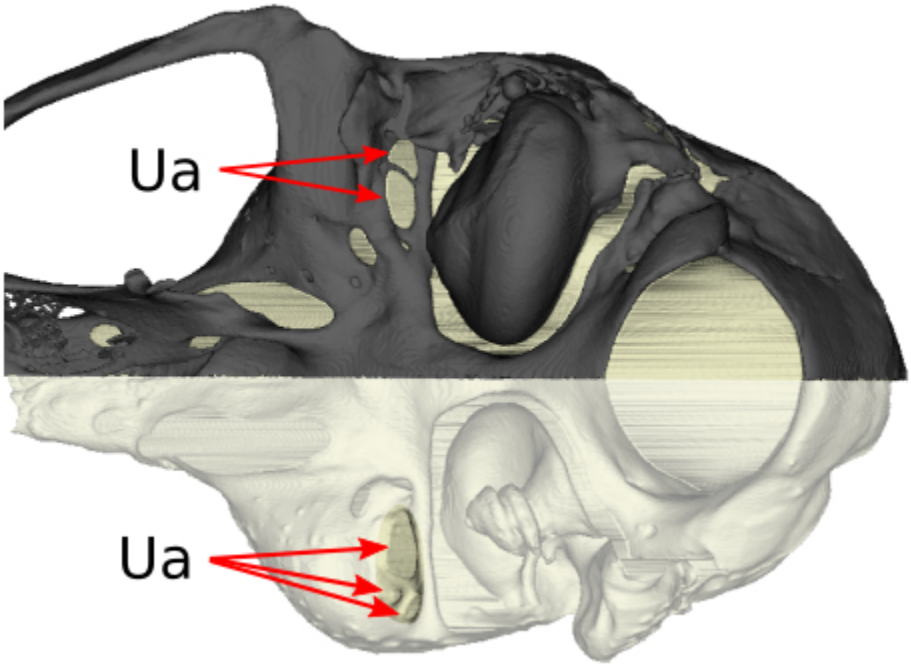

Figure 11: unknown apertures, also highlighting the difference in their number and shape between both sides

132x94mm (96 x 96 DPI)